Atmospheric
Chemistry
and Physics
Discussions

1 **The atmospheric impacts of monoterpene ozonolysis on**

2 **global stabilised Criegee intermediate budgets and SO$_2$**

3 **oxidation: experiment, theory and modelling**

4

5 **Mike J. Newland[1,3], Andrew R. Rickard[2,3], Tomás Sherwen[3], Mathew J. Evans[2,3],**

6 **Luc Vereecken[4,5], Amalia Muñoz[6], Milagros Ródenas[6], William J. Bloss[1]**

7 [1]{University of Birmingham, School of Geography, Earth and Environmental Sciences,
8 Birmingham, UK}

9  [2]{National Centre for Atmospheric Science (NCAS), University of York, York, UK}

10 [3]{Wolfson Atmospheric Chemistry Laboratories, Department of Chemistry, University of
11 York, York, UK}

12 [4]{Max Planck Institute for Chemistry, Atmospheric Sciences, Hahn-Meitner-Weg 1, Mainz,
13 Germany}

14 [5]{Institute for Energy and Climate Research, Forschungszentrum Jülich GmbH, Jülich,
15 Germany}

16 [6]{Fundación CEAM, EUPHORE Laboratories, Avda/Charles R. Darwin 14. Parque
17 Tecnologico, Valencia, Spain}

18 Correspondence to:   M. J. Newland (mike.newland@york.ac.uk)

19                          A. R. Rickard (andrew.rickard@york.ac.uk)

20

21 **Abstract**

22 The gas-phase reaction of alkenes with ozone is known to produce stabilised Criegee
23 intermediates (SCIs). These biradical/zwitterionic species have the potential to act as
24 atmospheric oxidants for trace pollutants such as SO$_2$, enhancing the formation of sulfate
25 aerosol with impacts on air quality and health, radiative transfer and climate. However, the
26 importance of this chemistry is uncertain as a consequence of limited understanding of the
27 abundance and atmospheric fate of SCIs. In this work we apply experimental, theoretical and
28 numerical modelling methods to quantify the atmospheric impacts, abundance, and fate, of

Atmospheric
Chemistry
and Physics
Discussions

Open Access

1   the structurally diverse SCIs derived from the ozonolysis of monoterpenes, the second most

2   abundant group of unsaturated hydrocarbons in the atmosphere. We have investigated the

3   removal of $SO_2$ by SCI formed from the ozonolysis of three monoterpenes ($\alpha$-pinene, $\beta$-

4   pinene and limonene) in the presence of varying amounts of water vapour in large-scale

5   simulation chamber experiments. The $SO_2$ removal displays a clear dependence on water

6   vapour concentration, but this dependence is not linear across the range of $[H_2O]$ explored. At

7   low $[H_2O]$ a strong dependence of $SO_2$ removal on $[H_2O]$ is observed, while at higher $[H_2O]$

8   this dependence becomes much weaker. This is interpreted as being caused by the production

9   of a variety of structurally (and hence chemically) different SCI in each of the systems

10   studied, each displaying different rates of reaction with water and of unimolecular

11   rearrangement/decomposition. The determined rate constants, $k(SCI+H_2O)$, for those SCI that

12   react primarily with $H_2O$ range from $4 - 310 \times 10^{-15}$ cm$^3$ s$^{-1}$. For those SCI that predominantly

13   react unimolecularly, determined rates range from $130 - 240$ s$^{-1}$. These values are in line with

14   previous results for the (analogous) stereo-specific SCI system of $syn$/$anti$-$CH_3CHOO$. The

15   experimental results are interpreted through theoretical studies of the SCI unimolecular

16   reactions and bimolecular reactions with $H_2O$, characterised for $\alpha$-pinene and $\beta$-pinene at the

17   M06-2X/aug-cc-pVTZ level of theory. The theoretically derived rates agree with the

18   experimental results within the uncertainties. A global modelling study, applying the

19   experimental results within the GEOS-Chem chemical transport model, suggests that > 98 %

20   of the total monoterpene derived global SCI burden is comprised of SCI whose structure

21   determines that they react slowly with water, and whose atmospheric fate is dominated by

22   unimolecular reactions. Seasonally averaged boundary layer concentrations of monoterpene-

23   derived SCI reach up to $1.2 \times 10^4$ cm$^{-3}$ in regions of elevated monoterpene emissions in the

24   tropics. Reactions of monoterpene derived SCI with $SO_2$ account for < 1 % globally but may

25   account for up to 50 % of the gas-phase $SO_2$ removal over areas of tropical forests, with

26   significant localised impacts on the formation of sulfate aerosol, and hence the lifetime and

27   distribution of $SO_2$.

28

29   **1   Introduction**

30   Chemical oxidation processes in the atmosphere exert a major influence on atmospheric

31   composition, leading to the removal of primary emitted species, and the formation of

32   secondary products. In many cases either the emitted species or their oxidation products

Atmospheric
Chemistry
and Physics
Discussions

1    negatively impact air quality and climate (e.g. ozone, which is also a potent greenhouse gas).

2    These reactions can also transform gas-phase species to the condensed phase, forming

3    secondary aerosol that again can be harmful to health and can both directly and indirectly

4    influence radiative transfer and hence climate (e.g. $SO_2$ oxidation leading to the formation of

5    sulfate aerosol).

6    Tropospheric gas-phase oxidants include the OH radical, ozone, the $NO_3$ radical, and halogen

7    atoms. Stabilised Criegee intermediates (SCIs), or carbonyl oxides, have been identified

8    as another potentially important oxidant in the troposphere (*e.g.* Cox and Penkett, 1971;

9    Mauldin et al., 2012). SCIs are thought to be formed in the atmosphere predominantly

10   from the reaction of ozone with unsaturated hydrocarbons, though other processes may

11   be important under certain conditions, e.g. alkyl iodide photolysis (Gravestock et al.,

12   2010), dissociation of the DMSO peroxy radical (Asatryan and Bozzelli, 2008).

13   Laboratory experiments and theoretical calculations have shown SCI to oxidise $SO_2$ (*e.g.*

14   Cox and Penkett, 1971; Welz et al., 2012; Taatjes et al., 2013), organic (Welz et al.,

15   2014) and inorganic (Foreman et al., 2016) acids (Vereecken et al., 2017), and a number

16   of other important trace gases found in the atmosphere, as well as forming adducts with

17   $NO_2$ (Taatjes et al., 2014; Vereecken et al., 2017; Caravan et al., 2017). Measurements in

18   a boreal forest (Mauldin et al., 2012) and at a coastal site (Berresheim et al., 2014) have

19   both identified a 'missing' process (in addition to reaction with OH) oxidising $SO_2$ to

20   $H_2SO_4$, potentially arising from SCI reactions.

21   Here, we present results from a series of experimental studies into SCI formation and

22   reactions, carried out under atmospheric boundary layer conditions in the European

23   Photochemical Reactor facility (EUPHORE), Valencia, Spain. We examine the ozonolysis of

24   three monoterpenes with very different structures (and hence reactivities with OH and ozone):

25   α-pinene (with an endocyclic double bond), β-pinene (with an exocyclic double bond) and

26   limonene (with both an endo and exo cyclic double bond). We observe the removal of $SO_2$ in

27   the presence of each alkene-ozone system as a function of water vapour concentration. This

28   allows us to derive relative SCI kinetics for reaction with $H_2O$, $SO_2$, and unimolecular

29   decomposition. Further, we calculate absolute unimolecular rates and bimolecular reaction

30   rates with $H_2O$ for all α-pinene and β-pinene derived SCI at the M06-2X/aug-cc-pVTZ level

31   of theory. A global modelling study, using the GEOS-Chem global chemical transport model,

1    is performed to assess global and regional impacts of the chemical kinetics of monoterpene

2    SCI determined in this study.

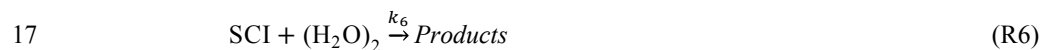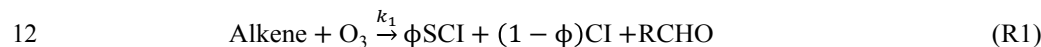## 1.1  Stabilised Criegee Intermediate Kinetics

4    Ozonolysis of an unsaturated hydrocarbon produces a primary ozonide that rapidly

5    decomposes to yield pairs of Criegee intermediates (CIs) and carbonyls (Johnson and

6    Marston 2008). The population of CIs are formed with a broad internal energy

7    distribution giving both chemically activated and stabilised forms. Chemically activated

8    CIs may undergo collisional stabilisation to an SCI, unimolecular decomposition or

9    isomerisation. SCIs can have sufficiently long lifetimes to undergo bimolecular reactions

10   (Scheme 1).

11   The predominant atmospheric fate for the simplest SCI, $CH_2OO$, is reaction with water

12   vapour (likely with the dimer (($H_2O)_2$) (e.g. Berndt et al., 2014; Newland et al., 2015a;

13   Chao et al., 2015; Lewis et al., 2015; Lin et al., 2016). For larger SCI, both experimental

14   (Taatjes et al., 2013; Sheps et al., 2014; Newland et al., 2015a; Huang et al., 2015) and

15   theoretical (Kuwata et al., 2010; Anglada et al., 2011; Anglada and Sole, 2016) studies

16   have shown that their kinetics, in particular reaction with water, are highly structure

17   dependent. The significant double bond character exhibited in the zwitterionic

18   configurations of mono-substituted SCI leads to two distinct chemical forms: *syn*-SCI

19   (*i.e.* those where an alkyl-substituent group is on the same side as the terminal oxygen of

20   the carbonyl oxide moiety)), and *anti*-SCI (*i.e.* with the terminal oxygen of the carbonyl

21   oxide moiety on the same side as a hydrogen group).  The two conformers of $CH_3CHOO$,

22   which are both mono-substituted, display these properties. This difference in conformer

23   reactivities has been predicted theoretically (Ryzhkov and Ariya, 2004, Kuwata et al.,

24   2010; Anglada et al., 2011; Lin et al., 2016) and was subsequently confirmed

25   experimentally (Taatjes et al., 2013; Sheps et al., 2014) for the two $CH_3CHOO$

26   conformers. The significantly faster reaction of *anti*-$CH_3CHOO$ with water is driven by

27   the higher potential energy of this isomer, while more stable SCI, with a methyl group in

28   *syn*-position, such as *syn*-$CH_3CHOO$ or $(CH_3)_2COO$, react orders of magnitude more

29   slowly with water.

30   SCI can also undergo unimolecular isomerisation/decomposition in competition with

31   bimolecular reactions. This is likely to be a significant atmospheric sink for *syn*-SCI because

Atmospheric
Chemistry
and Physics
Discussions

1    of their slow reaction with water vapour (e.g. Huang et al., 2015). Unimolecular reactions of

2    *syn*-CI/SCI are dominated by a 1,4-H-shift, forming a vinyl hydroperoxide (VHP)

3    intermediate (Niki et al., 1987; Rickard et al., 1999; Martinez and Herron, 1987; Johnson and

4    Marston, 2008; Kidwell et al., 2016). Decomposition of the VHP formed in this process is an

5    important non-photolytic source of OH, $HO_2$, and $RO_2$ in the atmosphere (Niki et al.,

6    1987; Alam et al., 2013; Kidwell et al., 2016), which can also lead to secondary organic

7    aerosol formation (Ehn et al., 2014). Unimolecular reactions of the *anti*-CI/SCI are

8    thought to be dominated by a 1,3-ring closure, the "acid/ester channel", in which the

9    CI/SCI decomposes, through a rearrangement to a dioxirane intermediate, producing a

10   range of daughter products and contributing to the observed overall $HO_x$ radical yield

11   (Kroll et al., 2002; Johnson and Marston, 2008; Alam et al., 2013).

12    $$\text{Alkene} + O_3 \xrightarrow{k_1} \phi\text{SCI} + (1-\phi)\text{CI} + \text{RCHO} \tag{R1}$$

13    $$\text{SCI} + SO_2 \xrightarrow{k_2} SO_3 + \text{RCHO} \tag{R2}$$

14    $$\text{SCI} + H_2O \xrightarrow{k_3} Products \tag{R3}$$

15    $$\text{SCI} \xrightarrow{k_d} Products \tag{R4}$$

16    $$\text{SCI} + acid \xrightarrow{k_5} Products \tag{R5}$$

17    $$\text{SCI} + (H_2O)_2 \xrightarrow{k_6} Products \tag{R6}$$

18   Decomposition of the simplest SCI, $CH_2OO$, is slow ($< 10$ $s^{-1}$) and is not likely to be an

19   important sink in the troposphere (e.g. Newland et al., 2015a; Chhantyal-Pun et al., 2015).

20   This decomposition occurs primarily via rearrangement through a 'hot' acid species, which

21   represents the lowest accessible decomposition channel (Gutbrod et al., 1996; Alam et al.,

22   2011; Chen et al., 2016). However, recently determined unimolecular reaction rates of larger

23   *syn*-SCI are considerably faster. Newland et al. (2015a) reported unimolecular reaction rate

24   constants for *syn*-$CH_3CHOO$ of 348 ($\pm$ 332) $s^{-1}$ and for $(CH_3)_2COO$ of 819 ($\pm$ 190) $s^{-1}$

25   (assuming $k(syn\text{-}CH_3CHOO+SO_2)$ = 2.9 $\times$ $10^{-11}$ $cm^3$ $s^{-1}$ (Sheps et al., 2014) and

26   $k((CH_3)_2COO+SO_2)$ = 1.3 $\times$ $10^{-10}$ $cm^3$ $s^{-1}$ (Huang et al., 2015), respectively). Smith et al.

27   (2016) measured the unimolecular decomposition rate of $(CH_3)_2COO$ to be 269 ($\pm$ 82) $s^{-1}$ at

28   283 K increasing to 916 ($\pm$ 56) $s^{-1}$ at 323 K, suggesting the rate to be fast and highly

29   temperature dependent. Novelli et al. (2014), estimated a significantly slower decomposition

Atmospheric
Chemistry
and Physics
Discussions

1    rate for *syn*-CH$_3$CHOO of 20 (3-30) s$^{-1}$ from direct observations of OH formation, while

2    Fenske et al. (2000), estimated the decomposition rate of CH$_3$CHOO (i.e. a mix of *syn* and

3    *anti* conformers) produced from ozonolysis of *trans*-but-2-ene to be 76 s$^{-1}$ (accurate to within

4    a factor of three).

5

6    **1.2   Monoterpene Ozonolysis**

7    Monoterpenes are volatile organic compounds (VOCs) with the general formula C$_{10}$H$_{16}$,

8    which are emitted by a wide range of vegetation, particularly from boreal forests. Total global

9    monoterpene emissions are estimated to be 95 (± 3) Tg yr$^{-1}$ (Sindelarova et al., 2014) -

10   roughly 13 % of total non-methane biogenic VOC emissions. Monoterpene emissions are

11   dominated by α-pinene, which accounts for roughly 34 % of the total global emissions, while

12   β-pinene and limonene account for 17 % and 9 % respectively (Sindelarova et al., 2014).

13   Monoterpenes (mainly α-pinene and limonene) are also present in indoor environments, in

14   significant amounts where cleaning products and air fresheners are in routine use (on the

15   order of 100s of ppbv) (e.g. Singer et al., (2006); Sarwar and Corsi, (2007)), where their

16   ozonolysis products can affect indoor chemistry and health (*e.g.* Rossignol et al., (2013);

17   Shallcross et al., (2014)).

18   Monoterpenes are highly reactive due to the presence of (often multiple) double bonds. The

19   oxidation of monoterpenes yields a wide range of multi-functional gas-phase and aerosol

20   products. This process can be initiated by OH and NO$_3$ radicals or by O$_3$, with ozonolysis

21   having been shown to be particularly efficient at generating low volatility products that can

22   form SOA, even in the absence of sulfuric acid (e.g. Ehn et al., 2014; Kirkby et al., 2016).

23   These highly oxygenated secondary products have received considerable attention in recent

24   years because of their role in affecting the climate through absorption and scattering of solar

25   radiation (the direct aerosol effect). They can also increase cloud condensation nuclei

26   concentrations, which can change cloud properties and lifetimes (the indirect aerosol effect).

27   They have also been shown to have a wide range of deleterious effects on human health (e.g.

28   Pöschl and Shiraiwa, 2015).

29   The ozonolysis reaction for monoterpenes is expected to follow a similar initial process to

30   that of smaller alkenes, with cyclo-addition at a double bond giving a primary ozonide (POZ),

31   followed by rapid decomposition of the POZ to yield a CI and a carbonyl (Scheme 1).

1    Stabilisation of the large POZs formed in monoterpene ozonolysis is expected to be

2    negligible (Nguyen et al., 2009). However, a major difference in ozonolysis at endocyclic

3    bonds is that, on decomposition of the POZ, the carbonyl oxide and carbonyl moieties are

4    tethered as part of the same molecule, providing the potential for further interaction of the

5    two. These can react together to form secondary ozonides (SOZ), which may be stable for

6    several hours (Beck et al., 2011). However, while this has been shown to be potentially the

7    major fate in the atmosphere for SCI derived from sesquiterpenes ($C_{15}H_{24}$) (e.g. Nguyen et al.,

8    2009b; Beck et al., 2011; Yao et al., 2014), formation of SOZ is predicted to be small for

9    monoterpene derived SCI because of the high ring strain caused by the tight cyclisation (e.g.

10   Nguyen et al., 2009b). Chuong et al. (2004) predicted formation of a SOZ to become the

11   dominant atmospheric fate for SCI formed in the ozonolysis of endo-cyclic alkenes with a

12   carbon number between 8 and 15, while Vereecken and Francisco (2012) suggested that

13   internal SOZ formation is likely to be limited to product rings containing six or more carbons

14   due to ring strain.

15   No studies have yet directly determined the reaction rates of the large SCI produced from

16   monoterpene ozonolysis with $SO_2$ (or any other trace gases). This is owing to the

17   complexities of synthesizing and measuring large SCI. However, Ahrens et al. (2014)

18   concluded that the reaction of the C9-SCI formed in β-pinene ozonolysis with $SO_2$ is as fast

19   as that determined by Welz et al. (2012) and Taatjes et al. (2013) for $CH_2OO$ and $CH_3CHOO$

20   respectively (ca. $4 \times 10^{-11}$ $cm^3$ $s^{-1}$) by fitting to the decay of $SO_2$ in the presence of the

21   ozonolysis reaction. Mauldin et al. (2012) calculated significantly slower reaction rates for an

22   additional oxidant (assumed to be SCI) derived from α-pinene and limonene ozonolysis, with

23   $k$(SCI+$SO_2$) determined to be $6 \times 10^{-13}$ $cm^3$ $s^{-1}$ and $8 \times 10^{-13}$ $cm^3$ $s^{-1}$ for α-pinene and limonene

24   derived SCI respectively. However, it seems likely that the rates calculated by Mauldin et al.

25   (2012) may be substantially underestimated due to the assumption of a very long SCI lifetime

26   (0.2 s) in experiments that were performed at 50 % RH. The calculated rates scale linearly

27   with SCI lifetime and based on reaction rates of smaller SCI with $H_2O$ (reported since the

28   Mauldin et al. work, e.g. Taatjes et al., 2013) it seems likely that the lifetime of the SCI in

29   their experiments would have been more like $0.1 - 2 \times 10^{-2}$ s, increasing the calculated rate

30   constants by more than an order of magnitude, bringing them into much closer agreement

31   with the rates reported by Ahrens et al. (2014).

32   Unimolecular reactions of the monoterpene SCI are expected to proceed rapidly through the

33   VHP route if a hydrogen is available for a 1,4 H-shift. Those SCI that cannot undergo this

1    rearrangement may undergo unimolecular reactions via the formation of the dioxirane

2    intermediate, but this is expected to be a much slower process (Nguyen et al., 2009). In

3    contrast to smaller SCI, it has been observed experimentally, and predicted theoretically, that

4    the VHP route will mainly lead to rearrangement to an acid (also yielding an OH radical)

5    rather than decomposition of the molecule (e.g. Ma et al., 2008, Ma and Marston, 2008). As

6    for the smaller alkenes, monoterpene ozonolysis has been shown to be a source of $HO_x$ (e.g.

7    Paulson et al., 1997; Alam et al., 2013), predominantly via the VHP rearrangement. The

8    MCMv3.3.1 (Jenkin et al., 2015) applies OH yields of 0.80, 0.35 and 0.87 for α-pinene, β-

9    pinene and limonene respectively.

### 1.2.1  α-pinene derived SCI

11    Decomposition of the α-pinene POZ yields four different $C_{10}$ Criegee intermediates (Scheme

12    2: CI-1a, 1b, 2a, 2b), with the carbonyl oxide moiety at one end and a carbonyl group at the

13    other. Here, CI-1 is a mono-substituted CI for which both *syn* (1a) and *anti* (1b) conformers

14    exist, while the other, CI-2, is di-substituted, for which two *syn*-conformers (2a and 2b) exist.

15    Ma et al. (2008) infer a relative yield of 50 % for the two basic CI formed, based on the

16    observation that norpinonic acid yields from the ozonolysis of α-pinene and an enone, which

17    upon ozonolysis yields CI-1, are almost indistinguishable.

18    The total SCI yield from α-pinene was determined to be 0.15 (± 0.07) by Sipilä et al. (2014)

19    in indirect experiments measuring the production of $H_2SO_4$ from $SO_2$ oxidation in the α-

20    pinene ozonolysis system. Drozd and Donahue (2011) also determined a total SCI yield of

21    about 0.15 at 740 Torr, from measuring the loss of hydrofluoroacetone in ozonolysis

22    experiments in a high pressure flow system. The MCMv3.3.1 (Jenkin et al., 1997; Saunders et

23    al., 2003; Jenkin et al., 2015) applies a value of 0.20 based on stabilisation of only the mono-

24    substituted CI-1.

### 1.2.2  β-pinene derived SCI

26    β-pinene ozonolysis yields two distinct conformers of the nopinone C9-CI (Scheme 3: CI-3

27    and CI-4), which differ in orientation of the carbonyl oxide group, and $CH_2OO$. CI-3 and CI-4

28    are formed in roughly equal proportions with very little inter-conversion between the two

29    (Nguyen et al., 2009). The difference in the chemical behaviour of CI-3 and CI-4, which were

30    often not distinguished in earlier studies, arises from the inability of the carbon attached to the

31    four-membered ring to undergo the 1,4-H-shift that allows unimolecular decomposition via

Atmospheric
Chemistry
and Physics
Discussions
Open Access
EGU

1   the VHP channel. This was noted in Rickard et al. (1999) as being a reason for the

2   considerably lower OH yield (obtained via the VHP route) from β-pinene ozonolysis

3   compared to that of α-pinene. This difference leads to contrasting unimolecular

4   decomposition rates for the two CI, with Nguyen et al. (2009) predicting a loss rate of *ca.* 50

5   $s^{-1}$ for CI-3 (via a VHP) and *ca.* 1 $s^{-1}$ for CI-4 (via ring closure to a dioxirane). This result is

6   qualitatively consistent with the experimental work of Ahrens et al. (2014), who determine a

7   ratio of 85:15 for the abundance of SCI-4:SCI-3 about 10 s after the initiation of the

8   ozonolysis reaction, as a consequence of the much faster decomposition rate of SCI-3. Thus

9   the potential for bimolecular reactions to compete with decomposition of SCI-3 and SCI-4 in

10  the atmosphere is very different.

11  Nguyen et al. (2009) theoretically calculate a total SCI yield from β-pinene ozonolysis of 42

12  %, consisting of 16.2 % SCI-3, 20.6 % SCI-4, and 5.1 % $CH_2OO$. Ahrens et al. (2014)

13  assume an equal yield of CI-3 and CI-4 (45 %) with a 10 % yield of $CH_2OO$; 40 % of the total

14  C9-CI are calculated to be stabilised at 1 atm. If all of the $CH_2OO$ is assumed to be formed

15  stabilised (e.g. Nguyen et al., 2009) then this gives a total SCI yield of 46 %. Earlier

16  experimental studies have tended to determine lower total SCI yields with Hasson et al.

17  (2001) reporting a total SCI yield of 0.27 from measured product yields (almost entirely

18  nopinone) and Hatakeyama et al. (1984) reporting a total SCI yield of 0.25. Winterhalter et al.

19  (2000) determined a yield of 0.16 (± 0.04) for excited $CH_2OO$ from β-pinene ozonolysis,

20  obtained via the nopinone yield and 0.35 for the stabilised C9-CI, giving a total SCI yield of

21  0.51 of all the $CH_2OO$ is assumed to be stabilised. Also, experimental studies have tended to

22  report higher $CH_2OO$ yields (determined from measured nopinone yields) than theoretical

23  studies. Nguyen et al. (2009) note that this could be because nopinone can also be formed in

24  bimolecular reactions of SCI-4, hence experimental studies may overestimate $CH_2OO$

25  production. The MCMv3.3.1 incorporates a total SCI yield of 0.25 from β-pinene ozonolysis,

26  with a yield of stabilised C9-CI of 0.102 and a $CH_2OO$ yield of 0.148.

27  ### 1.2.3  Limonene derived SCI

28  Limonene has two double bonds at which ozone can react. Theory suggests that reaction at

29  the endocyclic bond is more likely; Baptista et al. (2011) calculate reaction at the endo-cyclic

30  bond to be 84 – 94 % (dependent on the level of theory applied). Zhang et al. (2006) suggest

31  the reaction at the endo-cyclic double bond to be roughly 25 times faster than at the exo-

32  cyclic bond, i.e. leading to a branching ratio of ca. 96 % reaction at the endo bond and the

Atmospheric
Chemistry
and Physics
Discussions

1  current IUPAC recommendation (IUPAC, 2013) suggests about 95 % of the primary ozone

2  reaction to be at the endo bond. Leungsakul et al. (2005) reported a best fit to measurements

3  from chamber experiments by assuming an 85 % reaction at the endo-cyclic bond and 15 % at

4  the exo-cyclic bond.

5  Ozone reaction at the endo-cyclic bond of limonene produces four different $C_{10}$ CI (Scheme

6  4: CI-5a, 5b, 6a, 6b). Similar to CI-1 and CI-2 from α-pinene, CI-5 is a mono-substituted CI

7  for which both *syn* (5a) and *anti* (5b) conformers exist, while the other, CI-6, is di-substituted,

8  for which two *syn*-conformers (6a and 6b) exist. Leungsakul et al. (2005) determined a total

9  SCI yield from limonene ozonolysis of 0.34, consisting of $CH_2OO$ (0.05), CI-7 (0.04), CI-5

10  (0.15) and CI-6 (0.11). Sipilä et al. (2014) determined a total SCI yield of 0.27 (± 0.12) from

11  indirect experiments measuring the production of $H_2SO_4$ from $SO_2$ oxidation in the presence

12  of the limonene-ozone system. The MCMv3.3.1 describes only reaction with ozone at the

13  endocyclic double bond and recommends a total SCI yield of 0.135 with stabilisation of only

14  the mono-substituted CI-5.

15

16  **2  Experimental**

17  **2.1  Experimental Approach**

18  The EUPHORE facility is a 200 $m^3$ simulation chamber used primarily for studying reaction

19  mechanisms under atmospheric boundary layer conditions. Further details of the chamber

20  setup and instrumentation are available elsewhere (Becker, 1996; Alam et al., 2011), and a

21  detailed account of the experimental procedure, summarised below, is given in Newland et al

22  (2015a).

23  Experiments comprised time-resolved measurement of the removal of $SO_2$ in the presence of

24  the monoterpene-ozone system, as a function of humidity. $SO_2$ and $O_3$ abundance were

25  measured using conventional fluorescence and UV absorption monitors, respectively; alkene

26  abundance was determined via FTIR spectroscopy. Experiments were performed in the dark

27  (*i.e.* with the chamber housing closed; $j(NO_2) \leq 10^{-6}$ s$^{-1}$), at atmospheric pressure (*ca.* 1000

28  mbar) and temperatures between 287 and 302 K. The chamber is fitted with large horizontal

29  and vertical fans to ensure rapid mixing (*ca.* 2 minutes). Chamber dilution was monitored via

30  the first order decay of an aliquot of $SF_6$, added prior to each experiment. Cyclohexane (*ca.*

31  75 ppmv) was added at the beginning of each experiment to act as an OH scavenger, such that

Atmospheric
Chemistry
and Physics
Discussions

1    $SO_2$ reaction with OH was calculated to be $\leq 1$ % of the total chemical $SO_2$ removal in all

2    experiments.

3    Experimental procedure, starting with the chamber filled with clean scrubbed air, comprised

4    addition of $SF_6$ and cyclohexane, followed by water vapour, $O_3$ (*ca.* 500 ppbv) and $SO_2$ (*ca.*

5    50 ppbv). A gap of five minutes was left prior to addition of the monoterpene, to allow

6    complete mixing. The reaction was then initiated by addition of the monoterpene (*ca.* 400

7    ppbv for α-pinene and β-pinene, *ca.* 200 ppbv for limonene), and reagent concentrations

8    followed for roughly 30 - 60 minutes; *ca.* 30 − 90 % of the monoterpene was consumed after

9    this time, dependent on the reaction rate with ozone. Four α-pinene + $O_3$, five β-pinene + $O_3$,

10    and five limonene + $O_3$ experiments, as a function of $[H_2O]$, were performed in total. Each

11    individual run was performed at a constant humidity, with humidity varied to cover the range

12    of $[H_2O] = 0.1 − 19 \times 10^{16}$ molecules cm$^{-3}$, corresponding to an RH range of 0.1 − 28 % (at

13    298 K). Measured increases in $[SO_2]$ agreed with measured volumetric additions across the

14    $SO_2$ and humidity ranges used in the experiments (Newland et al., 2015a).

15    **2.2   Analysis**

16    A range of different SCI are produced from the ozonolysis of each of the three monoterpenes

17    (see Schemes 2 − 4), each with their own distinct chemical behaviour (*i.e.* yields, reaction

18    rates); it is therefore not feasible (from these experiments) to obtain data for each SCI

19    independently; consequently, for analytical purposes we necessarily treat the SCI population

20    in a simplified (lumped) manner – see Section 2.2.2.

21    SCI are assumed to be formed in the ozonolysis reaction with a yield ϕ (Reaction R1). They

22    can then react with $SO_2$, with $H_2O$, with acids formed in the ozonolysis reaction, with other

23    species present, or undergo unimolecular decomposition, under the experimental conditions

24    applied (Reactions R2 – R5). A fraction of the SCI produced reacts with $SO_2$. This fraction (*f*)

25    is the loss rate of the SCI to $SO_2$ ($k_2[SO_2]$) compared to the sum of the total loss processes for

26    the SCI (Equation E1) :

27
$$f = \frac{k_2[SO_2]}{k_2[SO_2] + k_3[H_2O] + k_d + k_5[\text{acid}] + \text{L}} \qquad \text{(E1)}$$

28    Here, *L* accounts for the sum of any other chemical loss processes for SCI in the chamber,

29    with the exception of reaction with acids these loss processes are expected to be negligible, as

1    discussed later. After correction for dilution, and neglecting other (non-alkene) chemical sinks

2    for $O_3$, such as reaction with $HO_2$ (also produced directly during alkene ozonolysis (Alam et

3    al., 2013; Malkin et al., 2010)), which was indicated through model calculations to account

4    for < 0.5 % of ozone loss under all the experimental conditions, the following equation is

5    derived:

6 $$\frac{dSO_2}{dO_3} = \phi.f \qquad \text{(E2)}$$

7    From Equation E2, regression of the loss of ozone ($dO_3$) against the loss of $SO_2$ ($dSO_2$) for an

8    experiment at a given RH determines the product $f.\phi$ at a given point in time. This quantity

9    will vary through the experiment as $SO_2$ is consumed, and other potential SCI co-reactants are

10    produced, as predicted by Equation E1. A smoothed fit was applied to the experimental data

11    for the cumulative consumption of $SO_2$ and $O_3$, $\Delta SO_2$ and $\Delta O_3$, (as shown in Figure 2) to

12    determine $dSO_2/dO_3$ (and hence $f.\phi$) at the start of each experiment, for use in Equation E2.

13    The start of each experiment (*i.e.* when $[SO_2] \sim 50$ ppbv) was used as this corresponds to the

14    greatest rate of production of the SCI, and hence largest experimental signals (*i.e.* greatest $O_3$

15    and $SO_2$ rate of change; greatest precision) and is the point at which the SCI + $SO_2$ reaction

16    has the greatest magnitude compared with any other potential loss processes for either

17    reactant species (see discussion below).

18    Other potential fates for SCIs include reaction with ozone (Kjaergaard et al., 2013; Vereecken

19    et al., 2014; Wei et al., 2014; Vereecken et al., 2015), with other SCI (Su et al., 2014;

20    Vereecken et al., 2014), carbonyl products (Taatjes et al., 2012), acids (Welz et al., 2014), or

21    with the parent alkene (Vereecken et al., 2014; Decker et al., 2017). Sensitivity analyses using

22    the most recent theoretical predictions (Vereecken et al., 2015) indicate that the reaction with

23    ozone may be significant under certain conditions, accounting for up to 7% of SCI loss for

24    *anti*-SCI (based on *anti*-$CH_3CHOO$) at the lowest RH (worst case) experiment. However,

25    generally SCI loss to ozone is calculated to be < 5% for *anti*-SCI and < 1% for *syn*-SCI.

26    Summed losses from reaction with SCI (self-reaction), carbonyls and alkenes are calculated to

27    account for < 1 % of the total SCI loss under the experimental conditions applied.

28    $CH_2OO$ and $CH_3CHOO$ have been shown to react rapidly ($k = 1 - 5 \times 10^{-10}$ cm$^3$ s$^{-1}$) with

29    formic and acetic acid (Welz et al., 2014). In ozonolysis experiments, Sipilä et al. (2014)

30    determined the relative reaction rate of acetic and formic acids with $(CH_3)_2COO$ (i.e. $k_5/k_2$) to

31    be roughly three. Organic acid mixing ratios in this work, as measured by FTIR, reached up to

Atmospheric
Chemistry
and Physics
Discussions

Open Access

EGU

1   a few hundreds of ppbv, suggesting these will likely be a significant SCI sink in our

2   experiments. We have therefore explicitly included reaction with organic acids in our

3   analysis, incorporating the uncertainty arising from the (unknown) acid reaction rate constant,

4   as described in Section 2.2.1.

5   To date, the effects of the water dimer, $(H_2O)_2$ on SCI removal have only been determined

6   experimentally for $CH_2OO$ (Berndt et al., 2014; Chao et al., 2015; Lewis et al., 2015;

7   Newland et al., 2015a). Theoretical calculations (Vereecken and Francisco, 2012) predicted

8   the significant effect of the water dimer compared to the monomer for $CH_2OO$, but also that

9   the ratio of the SCI + $(H_2O)_2$ : SCI + $H_2O$ rate constants, $k_5/k_3$, of the larger, more substituted

10  SCI, *anti*-$CH_3CHOO$ and $(CH_3)_2COO$, are 2 - 3 orders of magnitude smaller than for $CH_2OO$

11  (Vereecken and Francisco, 2012). This would make the dimer reaction negligible at

12  atmospherically accessible $[H_2O]$ (*i.e.* $< 1 \times 10^{18}$ cm$^{-3}$) for SCI larger than $CH_2OO$. Therefore,

13  the effect of the water dimer reaction with $C_{10}$– and $C_9$–SCI is not considered in this analysis.

14  For $CH_2OO$, the reaction rates with water and the water dimer have been quantified in recent

15  EUPHORE experimental studies, and the values from Newland et al. (2015a) are used.

16  **2.2.1 Derivation of $k$(SCI+$H_2O$)/$k$(SCI+$SO_2$) and $k_d$/$k$(SCI+$SO_2$)**

17  As noted above, a range of different SCI are produced from the ozonolysis of the three

18  monoterpenes (see Schemes 2 – 4), each with their own distinct chemical behaviour, which

19  treated individually, introduce too many unknowns (*i.e.* yields, reaction rates) for explicit

20  analysis. Consequently for analytical purposes we treat the SCI population in a simplified

21  (lumped) manner:

22  Firstly, we use the simplest model possible, assuming that a single SCI is formed in each

23  ozonolysis reaction (Equation E3).

$$\frac{f}{[SO_2]} = \left( [SO_2] + \frac{k_3}{k_2}[H_2O] + \frac{k_d}{k_2} + \frac{k_5}{k_2}[\text{acid}] \right)^{-1}$$

24                                                                                                                      (E3)

25  Secondly, for each monoterpene, the SCI produced are assumed to belong to one of two

26  populations, denoted SCI-A and SCI-B. These two populations are split according to the

27  observation that the decomposition rates and reaction rates with water for the smaller SCI

28  ($CH_3CHOO$) have been predicted theoretically (Ryzhkov and Ariya, 2004; Kuwata et al.,

29  2010; Anglada et al., 2011) and shown experimentally (Taatjes et al., 2013; Sheps et al.,

Atmospheric
Chemistry
and Physics
Discussions

1    2014; Newland et al., 2015a) to exhibit a strong dependence on the structure of the molecule.

2    The *syn*-CH$_3$CHOO conformer, which has the terminal oxygen of the carbonyl oxide moiety

3    in the *syn* position to the methyl group, has been shown to react very slowly with water and to

4    readily decompose, via the hydroperoxide mechanism; whereas the *anti*-CH$_3$CHOO

5    conformer, with the terminal oxygen of the carbonyl oxide moiety in the *anti*-position to the

6    methyl group, has been shown to react fast with water and is not able to decompose via the

7    hydroperoxide mechanism. Vereecken and Francisco (2012) have shown that all SCI studied

8    theoretically with an alkyl group in the *syn* position have reaction rates with H$_2$O of $k < 4 \times$

9    $10^{-17}$ molecule cm$^3$ s$^{-1}$ (and for SCI larger than acetone oxide, $k < 8 \times 10^{-18}$ molecule cm$^3$ s$^{-1}$).

10   We thus define two populations, assuming SCI-A (i.e. SCI that exhibit chemical properties of

11   the *anti*-type SCI) to react fast with water and not to undergo unimolecular reactions, and

12   SCI-B (i.e. SCI that exhibit chemical properties of the *syn* type SCI) to not react with water

13   but to undergo unimolecular reactions. This simplification allows us to fit to the

14   measurements using Equations E4 and E5, as shown below. The total SCI yields are

15   determined by our experiments at high SO$_2$, and the relative yields of SCI-A and SCI-B are

16   determined from fitting to Equation E5. These relative yields are then compared to those

17   predicted from the literature.

18   In this model, $f = \gamma^A f^A + \gamma^B f^B$, where $\gamma$ is the fraction of the total SCI yield (i.e. $\gamma^A + \gamma^B = 1$). $f^A$

19   and $f^B$ are the fractional losses of SCI-A and SCI-B to reaction with SO$_2$. Adapting Equation

20   E1 to include the two SCI species gives Equation E4, where $k_5[acid]$ accounts for the SCI +

21   acid reaction (see discussion of reaction rate constants below).

22
$$f = \frac{\gamma^A k_2^A [SO_2]}{k_2^A [SO_2] + k_3 [H_2O] + k_5^A [acid]} + \frac{\gamma^B k_2^B [SO_2]}{k_2^B [SO_2] + k_d + k_5^B [acid]} \quad \text{(E4)}$$

23   Equation E4 can be rearranged to Equation E5 and fitted according to $f/[SO_2]$ derived from

24   the measurements.

25
$$\frac{f}{[SO_2]} = \frac{\gamma^A}{[SO_2] + \frac{k_3}{k_2^A}[H_2O] + \frac{k_5^A}{k_2^A}[acid]} + \frac{\gamma^B}{[SO_2] + \frac{k_d}{k_2^B} + \frac{k_5^B}{k_2^B}[acid]} \quad \text{(E5)}$$

26   Using values for $\gamma^A$ and $\gamma^B$ from the literature and varying the assumed values of the reaction

27   of SCI with acid ($k_5$) allows us to determine $k_3/k_2^A$ and $k_d/k_2^B$.

Atmospheric
Chemistry
and Physics
Discussions

1    The assumptions made here allow analysis of a very complex system. However, a key

2    consequence is that the relative rate constants obtained from the analysis presented here are

3    not representative of the elementary reactions of any single specific SCI isomer formed, but

4    rather represent a quantitative ensemble description of the integrated system, under

5    atmospheric boundary layer conditions, which may be appropriate for atmospheric modelling.

6    Additionally our experimental approach cannot determine absolute rate constants (*i.e.* values

7    of $k_2$, $k_3$, $k_d$) in isolation, but is limited to assessing their relative values, measured under

8    atmospheric conditions, which may be placed on an absolute basis through use of an external

9    reference value (here the SCI + $SO_2$ rate constant).

## 2.2.2  SCI yield calculation

11   The value for the total SCI yield of each monoterpene, $\phi_{SCI\text{-}TOT}$, was determined from an

12   experiment performed under dry conditions (RH < 1%) in the presence of excess $SO_2$ (*ca.*

13   1000 ppbv), such that $SO_2$ scavenged the majority of the SCI. From Equation E2, regressing

14   $dSO_2$ against $dO_3$ (corrected for chamber dilution), assuming $f$ to be unity (*i.e.* all the SCI

15   produced reacts with $SO_2$), determines the value of $\phi_{min}$, a lower limit to the SCI yield. Figure

16   1 shows the experimental data, from which $\phi_{min}$ was derived.

17   In reality $f$ will be less than one, at experimentally accessible $SO_2$ levels, as a fraction of the

18   SCI may still react with trace $H_2O$ present, or undergo unimolecular reaction. The actual

19   yield, $\phi_{SCI}$, was determined by combining the result from the excess-$SO_2$ experiment with

20   those from the series of experiments performed at lower $SO_2$, as a function of $[H_2O]$, to obtain

21   $k_3/k_2$ and $k_d/k_2$ (see Section 2.2.1), through an iterative process to determine the single unique

22   value of $\phi_{SCI}$ which fits both datasets, as described in Newland et al. (2015a), but taking into

23   account the proposed model in this paper of there being two SCI produced. In this model, $f =$

24   $\gamma^A f^A + \gamma^B f^B$. Where $f^A = [SO_2] / ([SO_2] + k_3[H_2O]/k_2)$ and $f^B = [SO_2] / ([SO_2] + k_d/k_2)$ – other

25   possible SCI sinks are assumed to be negligible. In these excess-$SO_2$ experiments, $f^A \sim 1$ but

26   $f_B < 1$ since $k_d$ still represents a significant sink.

27   $\gamma^A$ (and hence $\gamma^B$, since $\gamma^B = 1 - \gamma^A$) is derived from fitting Equation E4 to the data from the

28   experiments performed at lower $SO_2$ for a given $\phi$. Using a range of $\phi$, gives a range of $\gamma$.

29   These different values of $\gamma$ are used with the respective values of $\phi$ in fitting to Equation E4

30   to determine values of $k_3/k_2$ and $k_d/k_2$.

31

## 3    Theoretical calculations

The rovibrational characteristics of all conformers of the CI formed from α-pinene and β-pinene, the transition states for their unimolecular reaction, and for their reaction with $H_2O$, were characterized quantum chemically, first using the M06-2X/cc-pVDZ level of theory, and subsequently refined at the M06-2X/aug-cc-pVTZ level. To obtain accurate barrier heights for reaction, it has been shown (Berndt et al., 2015; Chhantyal-Pun et al., 2017; Fang et al., 2016a, 2016b; Long et al., 2016; Nguyen et al., 2015) that post-CCSD(T) calculations are necessary. Unfortunately, performing such calculations for the SCI discussed in this paper, with up to 14 non-hydrogen atoms, is well outside our computational resources, though CCSD(T)/aug-cc-pVTZ single point energy calculations were performed for the unimolecular reactions of nopinone oxides and the most relevant subset of pinonaldehyde oxides. These data are sufficient for relative rate estimates, but it remains useful to improve the absolute barrier height predictions, using the data set by Vereecken et al. (Vereecken et al., 2017). This data set has a large number of systematic calculations on smaller CI, allowing empirical corrections to the DFT or CCSD(T) barrier heights to estimate the post-CCSD(T) barrier heights. The methodology for these corrections is described in more detail in Vereecken et al. (2017); briefly, it compares rate coefficient calculations against available harmonized experimental and very-high level theoretical kinetic rate predictions, and adjusts the barrier heights by 0.4 to 2.6 kcal mol$^{-1}$ (depending on the base methodology and the reaction type) to obtain best agreement with these benchmark results.

Using the energetic and rovibrational data thus obtained, multi-conformer transition state theory (MC-TST) calculations (Truhlar et al., 1996; Vereecken and Peeters, 2003) were performed to obtain the rate coefficient at 298K at the high pressure limit. All rate predictions incorporate tunnelling corrections using an asymmetric Eckart barrier (Eckart, 1930; Johnston and Heicklen, 1962). For the reaction of CI + $H_2O$, a pre-reactive complex is postulated at 7 kcal mol$^{-1}$ below the free reactants, while the CI + $(H_2O)_2$ reaction is taken to have a pre-reactive complex of 11 kcal mol$^{-1}$ stability. This pre-reactive complex affects tunnelling corrections; it is assumed that this pre-reactive complex is always in equilibrium with the free reactants.

In view of the high number of rotamers and the resulting computational cost, only a single limonene-derived CI isomer was studied, where the TS for the CI + $H_2O$ reaction was analyzed at the M06-2X/cc-pVDZ level of theory with only a partial conformational analysis;

Atmospheric
Chemistry
and Physics
Discussions

1   a limited number of the energetically most stable TS conformers thus discovered were re-

2   optimized at the M06-2X/aug-cc-pVTZ level of theory. These data will only be used for

3   qualitative assessments. However, we apply the structure-activity relationships (SARs)

4   presented by Vereecken et al. (Vereecken et al., 2017) to obtain an estimate of the rate

5   coefficients, and assess the role of the individual SCI isomers in limonene ozonolysis.

6   All quantum chemical calculations were performed using Gaussian-09 (Frisch et al., 2010).

7

8   **4   GEOS-Chem Model Simulation**

9   The global chemical transport model GEOS-Chem (v9-02, www.geos-chem.org, Bey et al.,

10   2002) is used to explore the spatial and temporal variability of the atmospheric impacts of the

11   experimentally derived chemistry. The model includes $HOx$-$NOx$-VOC-$O_3$-BrOx chemistry

12   (Mao et al., 2010; Parrella et al., 2012) and a mass-based aerosol scheme. Biogenic

13   monoterpene emissions are taken from the Model of Emissions of Gases and Aerosols from

14   Nature (MEGAN) v2.1 inventory (Guenther et al., 2006; 2012). Transport is driven by

15   assimilated meteorology (GEOS-5) from NASA's Global Modelling and Assimilation Office

16   (GMAO). The model is run at $4° \times 5°$ resolution, with the second year (2005) used for analysis

17   and first year discarded as spin up.

18   In this study, the standard simulation was expanded to include emissions of seven

19   monoterpene species (α-pinene, β-pinene, limonene, myrcene, ocimene, carene, and sabinene)

20   from MEGAN v2.1. The ozonolysis scheme for each monoterpene, detailed in Section 6.1,

21   considers the formation of one or two types of SCI, and their subsequent reaction with $SO_2$,

22   $H_2O$, or unimolecular decomposition. Reaction rate of the monoterpenes with OH, $O_3$ and

23   $NO_3$ rare detailed in Table S1.

24

25   **5   Results**

26   **5.1   SCI Yield**

27   Figure 1 shows the lower limit to the SCI yield, $\phi_{min}$, for the three monoterpenes, determined

28   from fitting Equation E5 to the experimental data. This gives values of 0.16 (± 0.01) for α-

29   pinene, 0.53 (± 0.01) for β-pinene and 0.20 (± 0.01) for limonene. These $\phi_{min}$ values were

30   then corrected as described in Section 2.2.2 using the $k_3/k_2$ and $k_d/k_2$ values determined from

Atmospheric
Chemistry
and Physics
Discussions

1   the measurements shown in Figures 3 – 5 using Equation E4. The corrected yields, $\phi_{SCI}$, are

2   0.19 (± 0.01) for α-pinene, 0.60 (± 0.03) for β-pinene and 0.23 (± 0.01) for limonene.

3   Uncertainties are ± 2σ, and represent the combined systematic (estimated measurement

4   uncertainty) and precision components. Literature yields for SCI production from

5   monoterpene ozonolysis are summarised in Table 1.

6   The value derived for the total SCI yield from α-pinene in this work of 0.19 agrees, within the

7   uncertainties, with the value of 0.15 (± 0.07) reported by Sipilä et al. (2014) and the value of

8   0.20 applied in the MCMv3.3.1.

9   The total SCI yield from β-pinene derived in this work, 0.60, agrees reasonably well with the

10  recent experimental work of Ahrens et al. (2014) who derived a total SCI yield of 0.50 (0.40

11  for the sum of CI-1 and CI-2 and 0.10 for $CH_2OO$, which is assumed to be formed almost

12  completely stabilised). The MCMv3.3.1 applies a total SCI yield of 0.25, of which 0.10 is a

13  C9-CI and 0.15 is $CH_2OO$. Earlier studies also tended to derive lower total SCI yields ranging

14  from 0.25 – 0.27 (Hasson et al., 2001; Hatakeyama et al., 1984).

15  The total SCI yield from limonene derived in this work, 0.23 (± 0.01) agrees with the recently

16  determined yield from Sipilä et al. (2014) of 0.27 (± 0.12). Leungsakul et al. (2005) derived a

17  somewhat higher yield of 0.34, while the MCMv3.3.1 applies a lower yield of 0.135.

## 5.2   $k_3(SCI+H_2O)/k_2(SCI+SO_2)$ and $k_d/k_2(SCI+SO_2)$ Analysis

19  Figure 2 shows the loss of $SO_2$ as ozone is consumed by reaction with the monoterpene for

20  each of the three systems. Box modelling results suggest that > 99 % of this $SO_2$ removal is

21  caused by reaction with SCI produced in the alkene-ozone reaction (rather than e.g. reaction

22  with OH, which is scavenged by cyclohexane). When the experiments are repeated at higher

23  relative humidity, the rate of loss of $SO_2$ decreases. This is as expected from Equation E1 and

24  suggests that there is competition between $SO_2$ and $H_2O$ for reaction with the SCI produced,

25  in agreement with observations of smaller SCI, which demonstrate the same competition

26  under atmospherically relevant conditions (Newland et al., 2015a; Newland et al., 2015b).

27  However, as the relative humidity is increased further, the $SO_2$ loss does not fall to (near) zero

28  as would be expected from Equation E1. This suggests that at high $[H_2O]$ the amount of $SO_2$

29  loss becomes less sensitive to $[H_2O]$. This is most likely due to there being at least two

30  chemically distinct SCI species present. This behaviour was previously observed for

1    CH$_3$CHOO by Newland et al. (2015a) and fits with the current understanding that the

2    reactivity of SCI is structure dependent.

3    To recap Section 2.2.1, the analysis presented here considers two models to fit the

4    observations. The first of these (Equation E3) assumes the formation of a single SCI species,

5    which, in addition to reacting with SO$_2$, can react with water, undergo unimolecular reaction

6    or react with acid. It is clearly evident from Figures 3 – 5 that this model does not give a good

7    fit to the observations for any of the monoterpene systems studied. Therefore, the results from

8    this (single SCI) approach are not discussed explicitly hereafter. The second of the models

9    (Equation E5) assumes the formation of two lumped, chemically distinct, populations of SCI,

10   denoted SCI-A and SCI-B. SCI-A is assumed to react fast with H$_2$O and to have minimal

11   decomposition. Conversely, SCI-B is assumed to have a negligible reaction with water under

12   the experimental conditions applied but to undergo rearrangement via a VHP. We use a least-

13   squares fit of Equation E5 to the data to determine the values of $k_3/k_2$ and $k_d/k_2$. This approach

14   fits the data well (Figures 3 - 5) for all 3 monoterpenes and represents the overall attributes of

15   the SCI formed - but as noted, does not represent an explicit determination of individual

16   conformer-dependent rate constants.

### 5.2.1 α-pinene

18   The α-pinene system is sensitive to water vapour at the low H$_2$O range, with the SO$_2$ loss

19   falling dramatically when the RH is increased from 0.1 to 2.5 % (Figure 2). However, at

20   higher RH the SO$_2$ loss appears to be rather insensitive to [H$_2$O].

21   CI-1 can be formed in either *syn* (1a) or *anti* (1b) configuration, whereas both CI-2

22   conformers formed are in a *syn* configuration (see Scheme 2). For one of the two conformers

23   of CI-2 (CI-2b), the hydrogen atom available for abstraction by the terminal oxygen of the

24   carbonyl oxide group is attached to the carbon on the four-membered ring. This has been

25   shown in the β-pinene system to make a large difference with respect to the ability of the

26   hydrogen to be abstracted and to undergo the VHP mechanism (Rickard et al., 1999; Nguyen

27   et al., 2009). This therefore suggests that CI-2b may exhibit characteristics of both SCI-A and

28   SCI-B. Ma et al. (2008) infer a probable equal yield of the two basic CI structures. This

29   would suggest a relative yield for SCI-A of 0.25 – 0.50 (depending on the precise nature of

30   CI-2b). Fitting Equation E4 to the data and allowing lambda to vary determines values of $\gamma^A$ =

31   0.40 and $\gamma^B$ = 0.60 (Figure 3).

Atmospheric
Chemistry
and Physics
Discussions

1    In Figure 3, Equation E4 is fitted to the α-pinene measurements, assuming

2    $k(\text{SCI+acid})/k(\text{SCI+SO}_2) = 0$. This derives a minimum value for $k(\text{SCI-A+H}_2\text{O})/k(\text{SCI-}$

3    $\text{A+SO}_2)$, the water dependent fraction of the SCI, and a maximum value for

4    $k(\text{decomposition:SCI-B})/k(\text{SCI-B+SO}_2)$, the water independent fraction of the SCI. The

5    kinetic parameters derived from the fitting are displayed in Table 2.

6    Figure 6 shows the variation of the derived $k_3/k_2$ and $k_d/k_2$ values as the ratio $k_5/k_2$,

7    $k(\text{SCI+acid})/k(\text{SCI+SO}_2)$, is varied from zero to one. The derived $k_3/k_2$ increases by about 40

8    % from $1.4\ (\pm 0.34) \times 10^{-3}$ to $2.0\ (\pm 0.49) \times 10^{-3}$. The derived $k_d/k_2$ value decreases, again by

9    about 40 %, from $8.2\ (\pm 1.5) \times 10^{12}\ \text{cm}^{-3}$ to $5.1\ (\pm 0.93) \times 10^{12}\ \text{cm}^{-3}$.

10   The derived limits to the relative rate constants can be put on an absolute scale using the

11   $k(\text{SCI+SO}_2)$ values for $\text{CH}_3\text{CHOO}$ from Sheps et al. (2014) for the *syn* and *anti* conformers.

12   These are, *syn*: $2.9 \times 10^{-11}\ \text{cm}^3\ \text{s}^{-1}$ and *anti*: $2.2 \times 10^{-10}\ \text{cm}^3\ \text{s}^{-1}$. The *syn* rate constant is applied

13   to the derived $k(\text{decomposition:SCI-B})/k(\text{SCI-B+SO}_2)$ value and the *anti* rate constant to the

14   $k(\text{SCI-A+H}_2\text{O})/k(\text{SCI-A+SO}_2)$ value. It should be noted that the $k_2$ values are for quite

15   different SCI to those formed in this study and to our knowledge no structure specific

16   $k(\text{SCI+SO}_2)$ have been reported for monoterpene derived SCI, though Ahrens et al. (2014)

17   determine an average $k_2 \sim 4 \times 10^{-11}\ \text{cm}^3\ \text{s}^{-1}$ for SCI derived from β-pinene, i.e. a value within

18   an order of magnitude of those determined for the smaller SCI $\text{CH}_2\text{OO}$, $\text{CH}_3\text{CHOO}$ and

19   $(\text{CH}_3)_2\text{COO}$ (e.g. Welz et al., 2012; Taatjes et al., 2013; Sheps et al., 2014; Huang et al.,

20   2015). Using the Sheps et al. (2014) values yields $k(\text{SCI-A+H}_2\text{O}) > 3.1\ (\pm 0.75) \times 10^{-13}\ \text{cm}^3\ \text{s}^{-}$

21   $^1$ and $k(\text{decomposition:SCI-B}) < 240\ (\pm 44)\ \text{s}^{-1}$ (using the values derived for $k(\text{SCI-}$

22   $\text{A+acid})/k(\text{SCI-A+SO}_2) = 0$). This $k_3$ value is an order of magnitude larger than the rate

23   constants determined for the smaller *anti*-$\text{CH}_3\text{CHOO}$ in the direct studies of Sheps et al.

24   (2014) $(2.4 \times 10^{-14}\ \text{cm}^3\ \text{s}^{-1})$ and Taatjes et al. (2013) $(1.0 \times 10^{-14}\ \text{cm}^3\ \text{s}^{-1})$. The decomposition

25   value derived for SCI-B is of the same order of magnitude as that for *syn*-$\text{CH}_3\text{CHOO}$ ($348 \pm$

26   $332\ \text{s}^{-1}$) and $(\text{CH}_3)_2\text{COO}$ ($819 \pm 190\ \text{s}^{-1}$) from Newland et al., (2015a) (using updated direct

27   measurement values of $k_2$ from Sheps et al. (2014) and Huang et al. (2015) for *syn*-

28   $\text{CH}_3\text{CHOO}$ and $(\text{CH}_3)_2\text{COO}$ respectively) and within the range from the recent paper by

29   Smith et al. (2016) which derives a decomposition rate for $(\text{CH}_3)_2\text{COO}$ of $269\ (\pm 82)\ \text{s}^{-1}$ at

30   283 K increasing to $916\ (\pm 56)\ \text{s}^{-1}$ at 323 K.

31   Sipilä et al. (2014) applied a single-SCI analysis approach to the formation of $\text{H}_2\text{SO}_4$ from

32   $\text{SO}_2$ oxidation in the presence of the α-pinene ozonolysis system. They determined that for α-

Atmospheric
Chemistry
and Physics
Discussions

1    pinene, $k_d \gg k(\text{SCI}+\text{H}_2\text{O})[\text{H}_2\text{O}]$ for $[\text{H}_2\text{O}] < 2.9 \times 10^{17}$ cm$^{-3}$, i.e. that the fate of SCI formed

2    in the system is rather insensitive to $[\text{H}_2\text{O}]$. Across the $[\text{SO}_2]$ and RH ranges used in their

3    study, the results obtained here would indicate $\text{H}_2\text{O}$ to always be the dominant sink for SCI-

4    A, i.e. the fact that Sipilä et al. (2014) see similar $\text{H}_2\text{SO}_4$ production across the RH range in

5    their study is consistent with these results.

6

### 5.2.2  β-pinene

8    Two recent studies (Nguyen et al., 2009; Ahrens et al., 2014) have suggested yields of the two

9    C$_9$-CI (CI-3 and CI-4, see Scheme 3) obtained from β-pinene ozonolysis to be roughly equal.

10   In these studies Ahrens et al. (2014) assume a $\text{CH}_2\text{OO}$ yield of 0.10 while Nguyen et al.

11   (2009) determine theoretically the yield of $\text{CH}_2\text{OO}$ to be 0.05. Another theoretical study

12   (Zhang and Zhang, 2005) predicted a $\text{CH}_2\text{OO}$ yield of 0.08. In experimental studies,

13   Winterhalter et al. (2000) determined the $\text{CH}_2\text{OO}$ yield to be 0.16 (± 0.04) from measuring

14   the nopinone yield and assuming it to be entirely a primary ozonolysis product (i.e. the co-

15   product of $\text{CH}_2\text{OO}$ formation) and Ma and Marston (2008) determine a summed contribution

16   of 84 % (± 0.03) for the two C$_9$-CI (i.e. a 16 % $\text{CH}_2\text{OO}$ yield). The theoretical studies are

17   somewhat lower than the experimental but Nguyen et al. (2009) note that CI-4 is likely to

18   form additional nopinone in bimolecular reactions. The $\text{CH}_2\text{OO}$ is assumed to all be formed

19   stabilised (e.g. Nguyen et al. 2009).

20   SCI-3 is expected to undergo unimolecular reactions at least an order of magnitude faster than

21   SCI-4 (Nguyen et al., 2009; Ahrens et al., 2014). The reaction of SCI-3 with water is expected

22   to be slow based on the calculations presented in Table 4, with a pseudo first order reaction

23   rate of 1.0 s$^{-1}$ at 75 % RH, 298 K, whereas the water reaction with SCI-4 is expected to be

24   considerably faster with a pseudo first order reaction rate of 240 s$^{-1}$ at 75 % RH, 298 K. This

25   reaction will thus likely be the dominant fate of SCI-4 at typical atmospheric RH. This is in

26   agreement with the observations of Ma and Marston (2008), that show a clear dependence of

27   nopinone formation on RH (presumed to be formed from SCI + $\text{H}_2\text{O}$). Fitting Equation E4 to

28   the data determines values of $\gamma^A = 0.41$ and $\gamma^B = 0.59$ (Figure 4).

29   Using these values, and assuming $k(\text{SCI}+\text{acid})/k(\text{SCI}+\text{SO}_2) = 0$, yields a $k(\text{SCI-}$

30   $\text{A}+\text{H}_2\text{O})/k(\text{SCI-A}+\text{SO}_2)$ value of $> 1.0$ (± 0.27) $\times 10^{-4}$ and a $k(\text{decomposition:SCI-B})/k(\text{SCI-}$

31   $\text{B}+\text{SO}_2)$ value of $< 6.0$ (± 1.3) $\times 10^{12}$ cm$^{-3}$ (Table 2).

Atmospheric
Chemistry
and Physics
Discussions

1  As shown in Figure 6, increasing $k_5/k_2$, $k(SCI+acid)/k(SCI+SO_2)$, from zero to one, decreases

2  the derived $k_d/k_2$ from 6.0 ($\pm$ 1.3) $\times$ $10^{12}$ cm$^{-3}$ to 1.8 ($\pm$ 0.39) $\times$ $10^{12}$ cm$^{-3}$. The derived $k_3/k_2$

3  increases by a factor of four from 1.0 ($\pm$ 0.27) $\times$ $10^{-4}$ to 3.7 ($\pm$ 1.0) $\times$ $10^{-4}$.

4  These values can be put on an absolute scale (using the values derived above for $k_5/k_2 = 0$).

5  For SCI-A, $k(SCI+SO_2)$ is taken as the experimentally determined value of 4 $\times$ $10^{-11}$ cm$^3$ s$^{-1}$

6  from Ahrens et al. (2014). For SCI-B, the $syn$-CH$_3$CHOO $k(SCI+SO_2)$ value determined by

7  Sheps et al. (2014) is used. This gives values of $k(SCI-A+H_2O) > 4 \times 10^{-15}$ ($\pm$ 1) cm$^3$ s$^{-1}$ and

8  $k(decomposition:SCI-B) < 170$ ($\pm$ 38) s$^{-1}$.

9  ## 5.2.3 Limonene

10  For the limonene measurements presented in Figure 2, $(dSO_2/dO_3)/dt$ appears to be non-

11  linear, with a jump in $dSO_2/dO_3$ between 120 and 150 ppbv of ozone consumed. This is most

12  evident in the two lowest RH runs (0.2 and 2.0 %). Limonene is the fastest reacting of the

13  systems presented here, with the alkene reaction having consumed 100 ppbv of ozone within

14  the first five minutes. The limonene sample required about five minutes of heating before the

15  entire sample was volatized and injected into the chamber. This therefore may account for the

16  apparent non-linear nature of $dSO_2/dO_3$ in Figure 2.

17  The SO$_2$ loss in the limonene-ozone system is less affected by increasing H$_2$O than for either

18  $\alpha$ or $\beta$-pinene (Figure 5), with the values of $f/[SO_2]$ (y-axis) varying by roughly a factor of two

19  over the RH range applied compared to more than a factor of three variation for the other two

20  systems. Hence it might be expected that there is little formation of H$_2$O dependent SCI or

21  that it has a rather slow reaction rate with water.

22  Fitting Equation E4 to the data determines values of $\gamma^A = 0.22$ and $\gamma^B = 0.78$ (Figure 5). This

23  is broadly in line with the ratio recommended in the MCMv3.3.1 of 0.27:0.73, and with that

24  proposed in Leungsakul et al. (2005) who use a CI-A:CI-B ratio of 0.35:0.65, but also include

25  some stabilisation of CH$_2$OO and C$_9$-CI from ozone reaction at the exo-cyclic bond. This

26  yields a $k(SCI-A+H_2O)/k(SCI-A+SO_2)$ value of $<$ 3.5 ($\pm$ 0.20) $\times$ $10^{-5}$ and a

27  $k(decomposition:SCI-B)/k(SCI-B+SO_2)$ value of $>$ 4.5 ($\pm$ 0.10) $\times$ $10^{12}$ cm$^{-3}$.

28  Figure 6 shows that the derived $k_d/k_2$ increases by about 7 % as $k(SCI+acid)/k(SCI+SO_2)$

29  ranges from 0.0 to 0.8. The derived $k_3/k_2$ becomes negative at $k(SCI+acid)/k(SCI+SO_2) > 0.8$,

30  putting an upper limit on this ratio, i.e. $k_5/k_2 < 0.8$, for the limonene system.

Atmospheric
Chemistry
and Physics
Discussions

1    Putting these values on an absolute scale (using the values derived for $k_5/k_2 = 0$), using the

2    $CH_3CHOO$ *syn* and *anti* $k(SCI+SO_2)$ determined by Sheps et al. (2014), yields values of $< 7.7$

3    $(\pm 0.60) \times 10^{-15}$ cm$^3$ s$^{-1}$ and $> 130$ ($\pm 3$) s$^{-1}$ for $k_3$ and $k_d$ respectively. These values are similar

4    to those derived for the SCI-A and SCI-B formed from β-pinene. The $k_3$ value is a factor of

5    three smaller than that determined by Sheps et al. (2014) for $k_3$(*anti*-$CH_3CHOO+H_2O$), $2.4 \times$

6    $10^{-14}$ cm$^3$ s$^{-1}$.

7    Sipilä et al. (2014) applied a single-SCI analysis approach to the formation of $H_2SO_4$ from

8    $SO_2$ oxidation by the limonene ozonolysis system and determined that, similarly to α-pinene,

9    $k$(decomp.) $\gg k$(SCI+ $H_2O$)[$H_2O$] for [$H_2O$] $< 2.9 \times 10^{17}$ cm$^{-3}$, i.e. that the system is rather

10    insensitive to [$H_2O$]. Our data are consistent with the limonene system being less sensitive to

11    [$H_2O$] than the SCI populations derived from the other two monoterpenes reported here.

12    ### 5.2.4 Experimental Summary

13    The removal of $SO_2$ in the presence of ozonolysis reactions of α-pinene, β-pinene and

14    limonene has been studied as a function of water vapour concentration, and analysed

15    following the approximation that the SCI population can be represented through a two species

16    model, with contrasting unimolecular decomposition rates and reactivity to water. The results

17    presented in this work suggest that all three monoterpenes studied produce a range of SCI that

18    have differing reactivities towards water and decomposition. This is in agreement with current

19    theoretical understanding but is the first experimental demonstration for large SCI derived

20    from monoterpene ozonolysis. The complex reactivity of the systems investigated is further

21    highlighted by the fact that the experimental data are not fitted well by the assumption of the

22    formation of a single SCI species. While the behaviour of large SCI derived from

23    monoterpenes are likely to be significantly more complicated than is accounted for by simply

24    considering the differing kinetics of *syn* and *anti* SCI conformers, this approach provides a

25    reasonable description of the experimental behaviour observed, and the results presented here

26    are broadly in line with experimental results from the smaller SCI and from theoretical

27    results. The reaction rates of SCI-A (i.e. SCI that exhibit chemical properties of the *anti*-type

28    SCI) derived from the three different monoterpenes with water range from $< 0.8$ to $> 31 \times 10^-$

29    $^{14}$ cm$^3$ s$^{-1}$, broadly in line with the derived rates of Sheps et al. (2014) for *anti*-$CH_3CHOO$ of

30    $2.4 \times 10^{-14}$ cm$^3$ s$^{-1}$. The decomposition rates of SCI-B (i.e. SCI that exhibit chemical

31    properties of the *syn*-type SCI) are on the order of 100 - 250 s$^{-1}$. This is in line with those

32    derived for *syn*-$CH_3CHOO$ from *cis* and *trans*-but-2-ene ozonolysis and $(CH_3)_2COO$ by

Atmospheric
Chemistry
and Physics
Discussions

1    Newland et al. (2015a) of 348 (± 332) s$^{-1}$ and 819 (± 190) s$^{-1}$ respectively (assuming $k(syn$-

2    CH$_3$CHOO+SO$_2$) = 2.9 × 10$^{-11}$ cm$^3$ s$^{-1}$ (Sheps et al., 2014) and $k$((CH$_3$)$_2$COO+SO$_2$) = 2.9 ×

3    10$^{-10}$ cm$^3$ s$^{-1}$ (Huang et al., 2015)) and recent results from Smith et al. (2016) of 269 – 916 s$^{-1}$

4    (strongly dependent on temperature) for (CH$_3$)$_2$COO decomposition. In this work we only

5    derive relative rates, but the similarity of the $k_3$ and $k_d$ values derived when the $k_2$ values for

6    $syn$ and $anti$-CH$_3$CHOO from Sheps et al. (2014) are applied is consistent with the recent

7    work of Ahrens et al. (2014), suggesting that large SCI, derived from monoterpenes,

8    demonstrate a similar reactivity towards SO$_2$ as smaller SCI. One uncertainty in the derivation

9    of the kinetics presented herein is the reactions of the SCI produced with organic acids. These

10   acids were present in the experiments (owing to formation in the monoterpene ozonolysis

11   reactions themselves) at levels which may have been a competitive sink for the SCI.

12   The ability of the simplified SCI-A / SCI-B approach to fit the experimental data and the

13   good agreement with theory and experimental work for smaller SCI suggests that the kinetic

14   parameters derived herein, using a lumped two-SCI system, may be useful for modelling and

15   provide the best available basis for modelling the effects of SCI on atmospheric SO$_2$

16   oxidation in the presence of water vapour. To this end, in Section 6 we present the results of a

17   global modelling study using the kinetic parameters derived herein.

18   **5.3    Theoretical results and comparison to experiments**

19   The theoretically predicted rate coefficients for unimolecular reactions of the monoterpene

20   SCI are listed in Table 3, while those for the reaction with H$_2$O are listed in Table 4. These

21   data can be compared against the experimental data obtained in this work.

22   5.3.1   α-pinene

23   The theory-based rate coefficients show one pinonaldehyde oxide, CI-1b, with a rate of

24   reaction with water that is significantly faster than the remaining α-pinene-derived CI.

25   Comparing this rate to the experimental data suggests that CI-1b corresponds to SCI-A, with

26   matching rate coefficients within an order of magnitude, i.e. within the expected uncertainty.

27   We thus deduce that SCI-A is CI-1b. The remaining pinonaldehyde oxides, CI-1a, CI-2a and

28   CI-2b, react predominantly through unimolecular reactions, where theory-based rate

29   coefficients range from 60 to 600 s$^{-1}$, all within a factor of 4 of the experimentally derived

30   population-averaged rate of 240 ± 44 s$^{-1}$, i.e. matching within the uncertainty margins. The

Atmospheric
Chemistry
and Physics
Discussions

1   unimolecular rate coefficients of this set of CI are sufficiently close that it is not feasible to

2   separate these in the experimental data, so we can only conclude that SCI-B in the α-pinene

3   ozonolysis experiments may consist of a mixture of C-1a, CI-2a and CI-2b.

### 5.3.2 β-pinene

5   The theoretical analysis for nopinone oxides shows one isomer, SCI-4, that has a fast rate of

6   reaction with water, but a slow unimolecular isomerisation, while the other isomer, SCI-3,

7   shows a fast unimolecular decomposition. These can thus be unequivocally equated to the

8   experimentally obtained SCI-A and SCI-B, respectively, inasmuch as the yield of $CH_2OO$ is

9   minor. The predicted rate coefficients are within the expected uncertainty intervals of the

10  theoretical data, a factor of 5 for the unimolecular rates, and an order of magnitude for the

11  reaction with $H_2O$.

12  The experimental rate measurements are defined relative to the reaction rate with $SO_2$; the

13  value adopted for the $k(SCI+SO_2)$ reaction therefore influences the derived rate coefficient

14  values. Ahrens et al. (2014) directly measured the $SO_2$ rate coefficient of the longest-lived

15  SCI (SCI-4) to be $\sim 4 \times 10^{-11}$ cm$^3$ s$^{-1}$, but for SCI-3 we assume a similar rate coefficient as

16  syn-$CH_3CHOO$ + $SO_2$ determined by Sheps et al. (2014) of $2.9 \times 10^{-11}$ cm$^3$ s$^{-1}$. Nopinone

17  oxides are bicyclic compounds, with a bulky dimethyl-substituted 4-membered ring adjacent

18  to the carbonyl oxide moiety. To examine the potential impact of steric hindrance on the SCI

19  + $SO_2$ reaction, we characterized all sulfur-substituted secondary ozonides (S-SOZ) formed in

20  this reaction (Kuwata et al., 2015; Vereecken et al., 2012). We find that the tri-cyclic S-SOZ

21  shows very little interaction between the sulfur-bearing ring and the β-pinene substituents,

22  and little change in ring strain. The energies of the S-SOZ adducts relative to the SCI + $SO_2$

23  reactants thus remains very similar to that of $CH_2OO$, $CH_3CHOO$ or $(CH_3)_2COO$, confirming

24  the quality of our selection of reference rate coefficients.

### 5.3.3 Limonene

26  Of the six non-$CH_2OO$ CI formed in limonene ozonolysis, CI-5b was predicted to have a fast

27  reaction rate with $H_2O$; its oxide substitution patterns is similar to pinonaldehyde oxide CI-1b.

28  The SAR-predicted rate coefficient of CI-5b + $H_2O$ is within a factor of 2 of the

29  experimentally derived $k_3$ value for SCI-A, such that we can equate SCI-A to CI-5b with

30  confidence. The SCI-B set of Criegee intermediates then contains the summed population of

31  the remaining five CI, all of which react slowly with $H_2O$. The SAR-predicted unimolecular

25

Atmospheric
Chemistry
and Physics
Discussions

1  decay rate coefficients range from 15 to 700 s$^{-1}$, all within a factor of 9 of the experimentally

2  obtained $k_d$ = 130 s$^{-1}$; it should be noted that for limonene-derived CI, no explicit theoretical

3  calculations are available, and the SAR-predictions carry a somewhat larger uncertainty.

4  We have performed an exhaustive characterisation of the conformers of CI-5b. The most

5  stable conformers show an internal complex formation between the oxide moiety and the

6  carbonyl group, similar to those characterized for the bimolecular reaction of CI with

7  carbonyl compounds (Jalan et al., 2013; Wei et al., 2015). The theoretical study by Jiang et al.

8  (2013) on limonene ozonolysis appears to have omitted internal rotation and cannot be

9  compared directly. It seems likely that the limonene-derived CI can thus easily undergo

10  internal SOZ formation, which is thought (Vereecken and Francisco, 2012) to be entropically

11  unfavourable, but to have a low barrier to reaction. For α-pinene, a similar internal complex

12  formation and SOZ ring closure is not as favourable due to the geometric limitations enforced

13  by the 4-membered ring.

14  A large number of transition state conformers for CI-5b + H$_2$O were characterized, though no

15  exhaustive search was completed. The energetically most favourable structures show

16  interaction between the carbonyl group, and the H$_2$O co-reactant as it adds onto the carbonyl

17  oxide moiety. Similar stabilising interactions between the carbonyl moiety and the

18  carbonyl oxide moiety were reported recently in cyclohexene-derived CI

19  (Berndt et al., 2017). This interaction thus lowers the barrier to reaction though it is currently

20  unclear whether it enhances the reaction rate compared to e.g. the α-pinene-derived CI-1b, as

21  these hydrogen-bonded structures are entropically not very favourable. The intra-molecular

22  interactions with heterosubstituents could be investigated in future work.

23

24  ## 6   Global modelling study

25  ### 6.1   SCI Chemistry

26  A global atmospheric modelling study was performed using the GEOS-Chem chemical

27  transport model (as described in Section 4) to examine the global monoterpene derived SCI

28  budget and the contribution of these SCI to gas-phase SO$_2$ oxidation. The existing chemistry

29  scheme in the model is supplemented with monoterpene SCI chemistry based on the

30  experimental results described in Section 5 and in Table 5. It should be noted here that this

31  modelling study focuses on the chemical impacts of monoterpene SCI formed from

Atmospheric
Chemistry
and Physics
Discussions

1 ozonolysis reactions only. No chemistry for other SCIs derived from isoprene and/or other

2 (smaller) alkenes are incorporated in the adapted model chemical scheme used.

3 The monoterpene emissions in GEOS-Chem are taken from MEGAN v2.1 (Guenther et al.,

4 2012). The scheme emits seven monoterpenes: α-pinene, β-pinene, limonene, myrcene,

5 ocimene, 3-carene, and sabinene. The monoterpenes are oxidised within the model by OH,

6 $NO_3$ and $O_3$ at rates shown in Table S1. Reaction with $O_3$ leads to the production of

7 monoterpene specific SCI. Reactions with OH and $NO_3$ does not lead to the formation of any

8 products, with the reactions only acting as a sink for the monoterpene and the respective

9 oxidant. The SCI yields from the ozonolysis of α-pinene, β-pinene, and limonene are derived

10 from the experimental work presented here. SCI from each monoterpene are split in to SCI-A

11 and SCI-B as defined in previous sections. For the other four monoterpenes emitted, the SCI

12 yields, and kinetics are derived based on similarity of structure to one of the species studied

13 here or previously in the literature. The main SCI produced in the ozonolysis of myrcene and

14 ocimene are expected to be acetone oxide ($(CH_3)_2COO$) or 4-vinyl-5-hexenal oxide

15 ($CH_2CHC(CH_2)CH_2CH_2CHOO$), since ozone has been suggested to react predominantly at

16 the isolated internal double bond (~97 % for myrcene, ~90% for ocimene (Baker et al.,

17 2004)). The SCI yield is taken to be 0.30, similar to that of $(CH_3)_2COO$ from 2,3-dimethyl-

18 but-2-ene ozonolysis (Newland et al., 2015a). However, this may be an underestimate since it

19 has been predicted that stabilisation of small CI increases with an increasing size of carbonyl

20 co-product, as this co-product can take more of the nascent energy of the primary ozonide on

21 decomposition due to a greater number of degrees of freedom available (Nguyen et al., 2009,

22 Newland et al., 2015b). Sabinene is a bicyclic monoterpene with an external double bond and

23 hence is treated like β-pinene. This assumption is backed up by recent theoretical work (Wang

24 and Wang, 2017), who predict similar behaviour of sabinene derived SCI to the predicted

25 behaviour of β-pinene SCI by Nguyen et al. (2009a). They predict a SCI yield between 24 % -

26 64 %. 3-carene is a bicyclic monoterpene with an internal double bond and is treated like α-

27 pinene.

28 **6.2 Modelling Results**

29 Figure 7 shows the annually averaged total SCI burden from monoterpene ozonolysis in the

30 surface layer in the GEOS-Chem simulation. A number of interesting features are apparent

31 from this figure and the associated information given in Table 6:

1      (i)     The highest annually averaged monoterpene SCI concentrations are found

2             above tropical forests.

3      (ii)    Peak anually averaged monoterpene SCI concentrations are $\sim 1.2 \times 10^4$ cm$^{-3}$.

4      (iii)   > 97 % of the total monoterpene SCI burden is SCI-B.

5    Annual global monoterpene emissions are dominated by the tropics (Figure S1), accounting

6    for > 90 % during the northern hemisphere winter months (November – April) and 70 % even

7    during the peak emissions from the northern boreal region during June and July (Sindelarova

8    et al., 2014). Despite annually averaged surface ozone mixing ratios being roughly a factor of

9    2 higher in the northern mid-high latitudes, monoterpene SCI production is still dominated by

10   the tropics. Annually averaged surface monoterpene SCI concentrations across the northern

11   boreal regions are $< 2 \times 10^3$ cm$^{-3}$; during the summer months (JJA) this value rises to $2 - 5 \times$

12   $10^3$ cm$^{-3}$.

13   More than 97 % of the total monoterpene derived SCI are SCI-B (Table 6). This is because

14   typical water vapour concentrations in the tropics are $> 5.0 \times 10^{17}$ cm$^{-3}$. This gives SCI-A

15   removal rates (i.e. $k_3$[H$_2$O]) of $2 \times 10^3 - 1.5 \times 10^5$ s$^{-1}$, whereas removal rates of SCI-B to

16   unimolecular reactions have been determined here to be $1 - 3$ orders of magnitude slower, on

17   the order of 100 - 250 s$^{-1}$. Since the loss of SCI-B is independent of temperature in the model,

18   the highest SCI-B concentrations would be expected to be located in the regions of highest

19   SCI-B production. Recent experimental studies (Smith et al., 2016) have demonstrated a

20   strong temperature dependence for the unimolecular decomposition rate of (CH$_3$)$_2$COO

21   between 283 and 323 K ($269 - 916$ s$^{-1}$). Therefore, it may be that in reality there would be

22   some geographical variation in the rate of unimolecular loss.

23   The monoterpene SCI-A + H$_2$O reactions are expected to lead to high yields of both large

24   (e.g. Ma et al., 2008; Ma and Marston, 2008) and small (measured in high yield in the

25   experiments presented here) organic acids.

26   Figure 8 shows the seasonal removal of SO$_2$ by reaction with monoterpene derived SCI, as a

27   percentage of total gas-phase SO$_2$ oxidation in the surface layer. Monoterpene SCI are most

28   important (relative to OH) for SO$_2$ oxidation over tropical forests, where they account for up

29   to 50 % of the local gas-phase SO$_2$ removal during DJF and MAM in some regions. The

30   reasons for this are two-fold: firstly, the highest modelled monoterpene SCI concentrations

31   are found in these regions (Figure 7); but additionally, OH concentrations in the model are

32   low over these areas (Figure S2). Historically there has been discrepancies between modelled

Atmospheric
Chemistry
and Physics
Discussions

1    and observed OH concentrations over tropical forests, with models appearing to under-predict

2    [OH] by up to a factor of ten (e.g. Lelieveld et al., 2008). It was proposed that this was due to

3    missing sources of OH recycling during isoprene oxidation. During recent years there have

4    been advances in our understanding of isoprene chemistry. GEOS-Chem v-09, used here,

5    includes an isoprene OH recycling scheme largely based on Paulot et al. (2009a, 2009b), with

6    updates from Peeters et al. (2009), Peeters and Müller (2010), and Crounse et al. (2011;

7    2012), and evaluated in Mao et al. (2013). However, more recent experimental and theoretical

8    work is not yet included.

9    Annually, monoterpene SCI oxidation accounts for 1.1 % of the gas-phase $SO_2$ oxidation in

10   the terrestrial tropics. This accounts for the removal of 2.5 Gg of $SO_2$. Across the northern

11   boreal forests, monoterpene SCI contribute 0.5 % to gas-phase $SO_2$ removal annually,

12   removing 0.6 Gg of $SO_2$. Globally, throughout the whole atmosphere, monoterpene SCI

13   account for only 0.4 % of gas-phase $SO_2$ removal, removing 6.8 Gg of $SO_2$ annually.

14   It is noted that MEGAN does not contain oceanic monoterpene emissions, which may

15   increase the global importance of SCI for gas-phase $SO_2$ removal. Luo and Yu (2010)

16   determined annual global oceanic α-pinene emissions to be 29.5 TgC using a top-down

17   approach, with only 0.013 (Luo and Yu, 2010) – 0.26 (Hackenberg et al., 2017) TgC

18   estimated using a range of bottom-up approaches; clearly there are large uncertainties in

19   oceanic monoterpene emissions. At the upper end of this range they could potentially provide

20   a similar contribution to SCI production and subsequent $SO_2$ oxidation as monoterpenes

21   emitted from the terrestrial biosphere. SCI production more generally could be further

22   amplified by sources such as marine-derived alkyl iodine photolysis.

23   Blitz et al. (2017) recently calculated a revised $SO_2$ + OH reaction rate ($k_1$ (1 bar $N_2$) (298 K)

24   = 5.8 × $10^{-13}$ $cm^3$ $s^{-1}$), based on experimental work and a master equation analysis, which is ~

25   40 % lower than the rate given in the most recent JPL data evaluation (Burkholder et al.,

26   2015) (($k_1$ (1 bar $N_2$) (298 K) = 9.5 × $10^{-13}$ $cm^3$ $s^{-1}$), which is used in the GEOS-Chem model

27   simulation.  Figure S3 shows the increased influence of monoterpene derived SCI on gas-

28   phase $SO_2$ oxidation if the alternative $SO_2$ + OH rate is used. This increased the impact of

29   monoterpene SCI to up to 60 % of gas-phase $SO_2$ removal in regions of the tropical forests

30   during DJF and MAM, with the contribution of monoterpene SCI to global gas-phase $SO_2$

31   oxidation increasing to 0.6 %.

1    While certain monoterpenes appear to be more important than others with regard to the

2    production of SCI which will oxidise $SO_2$, these results are sensitive to the kinetics used and

3    the assumptions made for the monoterpenes not studied experimentally here. Hence we do not

4    attempt to draw any conclusions about the relative importance of each monoterpene from the

5    modelling. Clearly the most important monoterpenes will be those with high yields of SCI-B,

6    particularly if those SCI-B have a structure that hinders unimolecular decomposition (such as

7    certain β-pinene derived SCI).

8

9    **7    Discussion and Atmospheric Implications**

10   Monoterpene ozonolysis produces a diverse range of SCIs, with contrasting fates in the

11   atmosphere, dominated by unimolecular reaction or reaction with water vapour, but which

12   may still affect atmospheric $SO_2$ processing.  Monoterpene-derived SCI have the potential to

13   make a significant contribution to gas-phase $SO_2$ oxidation in specific local (i.e. forested)

14   environments, of up to 50 % at certain times of year - amplifying sulfate aerosol formation,

15   reducing the atmospheric lifetime and hence geographic distribution of $SO_2$, however the

16   results presented here show that their impact upon annual $SO_2$ oxidation globally is modest.

17   The results presented here demonstrate that it is important that monoterpene ozonolysis

18   reactions are considered to produce at least two different SCI species if their chemistry is to

19   be adequately represented in global models. This is because even a 'moderate' reaction rate

20   with water would be a dominant sink of an SCI with the averaged properties of SCI-A and

21   SCI-B.

22   SCI concentrations are expected to vary greatly depending on the local environment and time

23   of year, *e.g.* monoterpene abundance may be considerably higher (and with a different

24   reactive mix of alkenes giving a range of structurally diverse SCI) in a forested environment,

25   compared to a rural background. Furthermore, biogenic isoprene and monoterpene emissions

26   are strongly temperature dependent, hence are predicted to change significantly in the future

27   as a response to a changing climate and other environmental conditions (Peñuelas and Staudt,

28   2010).

29   This study shows that the ozonolysis of monoterpenes may contribute to significant SCI

30   concentrations in forested areas. Another group of compounds produced by forests that may

31   also have the potential to be a significant source of SCI are sesquiterpenes ($C_{15}H_{24}$). Although

1    generally present at low mixing ratios, this is due to their short atmospheric lifetimes caused

2    by their rapid reaction rates with ozone. The flux through the alkene-ozone reaction for fast

3    reacting monoterpenes and sesquiterpenes is often higher than for monoterpenes with high

4    mixing ratios but low removal rates, e.g. α-pinene and β-pinene. Ozonolysis of sesquiterpenes

5    has been shown to have very high SCI yields (Beck et al., 2011; Yao et al., 2014) and these

6    SCI have been shown to react with SCI scavengers (e.g. $SO_2$, $H_2O$ etc.) in a similar way to

7    smaller SCI (Yao et al., 2014). It has been predicted that SCI from sesquiterpenes may have a

8    high degree of secondary ozonide formation (Chuong et al., 2004) but experimental work has

9    shown very different results for structurally different sesquiterpenes studied (Beck et al.,

10   2011; Yao et al., 2014) hence this is highly uncertain, as is the fate of the SOZ once formed.

11   Therefore, these have the potential to be another significant source of SCI.

12

## 8    Conclusions

14   We report results from an integrated experimental (simulation chamber), theoretical (quantum

15   chemical) and modelling (global chemistry-transport simulation) study of the impacts of

16   monoterpene ozonolysis reactions on stabilised Criegee intermediate (SCI) formation and $SO_2$

17   oxidation.  The ozonolysis of the monoterpenes α-pinene, β-pinene and limonene have been

18   shown to produce a structurally diverse range of chemically distinct SCIs, with some showing

19   limited sensitivity to / reaction with water vapour under near-atmospheric humidity levels. A

20   multi-component system is required to explain the experimentally observed $SO_2$ removal

21   kinetics. A two-body model system based on the assumption of a fraction of the SCI produced

22   being reactive towards water (SCI-A; potentially contributing to the significant formation of a

23   range of organic acids in the atmosphere), and a fraction being relatively unreactive towards

24   water (SCI-B), analogous to the structural dependencies observed for the simpler $CH_3CHOO$

25   SCI system, has been shown to describe the observed kinetic data reasonably well for all the

26   monoterpene systems investigated, and may form a computationally affordable and

27   conceptually accessible basis for the description of this chemistry within atmospheric models.

28   The atmospheric fate of SCI-B produced from the monoterpenes studied here will be

29   controlled by their removal by unimolecular decomposition. In this work, we have

30   experimentally determined the monoterpene SCI-B decomposition rate to be between 100 and

31   250 $s^{-1}$. This has significant implications for the role of monoterpene derived SCI as oxidants

32   in the atmosphere. The fate of SCI-A will be reaction with water or the water dimer, likely

33   leading to the production of a range of organic acids.

Atmospheric
Chemistry
and Physics
Discussions

Open Access

EGU

1    A theory-based analysis of the kinetics of the SCI formed from α-pinene, β-pinene ozonolysis

2    has also been performed, which complements the experimental work. The identification of the

3    likely SCI-A and SCI-B populations and the derived kinetics agree with experimental

4    observations within the respective uncertainties.

5    A modelling study using the GEOS-Chem global 3-D chemical transport model supplemented

6    with the chemical kinetics elucidated in this work suggests that the global monoterpene

7    derived SCI burden will be dominated (> 97%) by SCI-B. The highest annually averaged SCI

8    concentrations are found in the tropics, with seasonally averaged monoterpene SCI

9    concentrations up to $1.2 \times 10^4$ cm$^{-3}$ owing to large monoterpene emissions. Across the boreal

10   forest, average SCI concentrations reach between $3 - 5 \times 10^3$ cm$^{-3}$ during the northern

11   hemisphere summer. Oxidation of $SO_2$ by monoterpene SCI is shown to also be most

12   important in the tropics. While oxidation by SCI contributes < 1% to gas-phase $SO_2$ oxidation

13   globally, over tropical forests this can rise to up to 50 % at certain times of the year.

14   Monoterpene SCI driven $SO_2$ oxidation will increase the production of sulfate aerosol –

15   affecting atmospheric radiation transfer, and hence climate; and reduce the atmospheric

16   lifetime and hence transport of $SO_2$. These effects will be substantial in areas where

17   monoterpene emissions are significant, in particular over the Amazon, Central Africa and SE

18   Asian rainforests.

19

20

21   **Data Availability**

24

25   **Acknowledgements**

Atmospheric
Chemistry
and Physics
Discussions

# 1 References

2 Ahrens, J., Carlsson, P. T. M., Hertl, N., Olzmann, M., Pfeifle, M., Wolf, J. L., and Zeuch, T.:

3 Infrared Detection of Criegee Intermediates Formed during the Ozonolysis of β-pinene and

4 Their Reactivity towards Sulfur Dioxide, Angew. Chem. Int. Ed. Engl., **53**, 715–719, 2014.

5 Alam, M. S., Camredon, M., Rickard, A. R., Carr, T., Wyche, K. P., Hornsby, K. E., Monks,

6 P. S., and Bloss, W. J.: Total radical yields from tropospheric ethene ozonolysis, Phys. Chem.

7 Chem. Phys., 13, 11002–11015, 2011.

8 Alam, M. S., Rickard, A. R., Camredon, M., Wyche, K. P., Carr, T., Hornsby, K. E., Monks,

9 P. S., and Bloss, W. J.: Radical Product Yields from the Ozonolysis of Short Chain

10 Alkenes under Atmospheric Boundary Layer Conditions, J. Phys. Chem. A, 117, 12468-

11 12483, 2013.

12 Anglada, J. M., Gonzalez, J., and Torrent-Sucarrat, M.: Effects of the substituents on the

13 reactivity of carbonyl oxides. A theoretical study on the reaction of substituted carbonyl

14 oxides with water, Phys. Chem. Chem. Phys., 13, 13034–13045, 2011.

15 Anglada, M. and Sole, A.: Impact of the water dimer on the atmospheric reactivity of

16 carbonyl oxides, Phys. Chem. Chem. Phys., 18, 17698-17712, 2016.

17 Asatryan, R. and Bozzelli, J.W.: Formation of a Criegee intermediate in the low-temperature

18 oxidation of dimethyl sulfoxide, Phys. Chem. Chem. Phys., 10, 1769–1780, 2008.

19 Baptista, L., Pfeifer, L., da Silva, E. C., and Arbilla, G.: Kinetics and Thermodynamics of

20 Limonene Ozonolysis, J. Phys. Chem. A, 115, 10911-10919, 2011.

21 Beck, M., Winterhalter, R., Herrmann, F., and Moortgat, G. K.: The gas-phase ozonolysis of

22 α-humulene, Phys. Chem. Chem. Phys., 13, 10970–11001, 2011.

23 Becker, K. H.: EUPHORE: Final Report to the European Commission, Contract EV5V-

24 CT92-0059, Bergische Universität Wuppertal, Germany, 1996.

25 Berndt, T., Voigtländer, J., Stratmann, F., Junninen, H., Mauldin III, R. L., Sipilä, M.,

26 Kulmala, M., and Herrmann, H.: Competing atmospheric reactions of $CH_2OO$ with $SO_2$ and

27 water vapour, Phys. Chem. Chem. Phys., 16, 19130–19136, 2014.

28 Berndt, T., Kaethner, R., Voigtländer, J., Stratmann, F., Pfiefle, M., Reichle, P., Sipilä, M.,

29 Kulmala, M., and Olzmann, M.: Kinetics of the unimolecular reaction of $CH_2OO$ and the

Atmospheric
Chemistry
and Physics
Discussions

1    bimolecular reactions with the water monomer, acetaldehyde and acetone at atmospheric

2    conditions, Phys. Chem. Chem. Phys., 17, 19862–19873, 2015.

3    Berndt, T., Herrmann, H. and Kurtén, T.: Direct probing of Criegee intermediates from gas-

4    phase ozonolysis using chemical ionization mass spectrometry, J. Am. Chem. Soc., DOI:

5    10.1021/jacs.7b05849, 2017.

6    Berresheim, H., Adam, M., Monahan, C., O'Dowd, C., Plane, J. M. C., Bohn, B., and Rohrer

7    F.: Missing $SO_2$ oxidant in the coastal atmosphere? – observations from high-resolution

8    measurements of OH and atmospheric sulfur compounds, Atmos. Chem. Phys., 14, 12209-

9    12223, 2014.

10   Bey, I., Jacob, D. J., Yantosca, R. M., Logan, J. A., Field, B. D., Fiore, A. M., Li, Q., Liu, H.

11   Y., Mickley, L. J., and Schultz, M. G.: Global modelling of tropospheric chemistry with

12   assimilated meteorology: Model description and evaluation, J. Geophys. Res., 106, 23073–

13   23095, 2001.

14   Blitz, M. A., Salter, R. J., Heard, D. E., and Seakins, P. J.: An Experimental and Master

15   Equation Study of the Kinetics of OH/OD + $SO_2$: The Limiting High-Pressure Rate

16   Coefficients, J. Phys. Chem. A, 121, 3184-3191, 2017.

17   J. B. Burkholder, S. P. Sander, J. Abbatt, J. R. Barker, R. E. Huie, C. E. Kolb, M. J. Kurylo,

18   V. L. Orkin, D. M. Wilmouth, and P. H. Wine "Chemical Kinetics and Photochemical Data

19   for Use in Atmospheric Studies, Evaluation No. 18," JPL Publication 15-10, Jet Propulsion

20   Laboratory, Pasadena, 2015 http://jpldataeval.jpl.nasa.gov.

21   Caravan, R. L., Khan, A. H. M., Rotavera, B., Papajak, E., Antonov, I. O., Chen, M. -W., Au,

22   K., Chao, W., Osborn, D. L., Lin, J. J. -M., Percival, C. J., Shallcross, D. E., and Taatjes, C.

23   E.: Products of Criegee intermediate reactions with $NO_2$: experimental measurements and

24   tropospheric implications, Faraday Discuss., 200, 313-330, 2017.

25   Chao, W., Hsieh, J. -T., Chang, C. -H., and Lin, J. J. -M.: Direct kinetic measurement of the

26   reaction of the simplest Criegee intermediate with water vapour, Science, DOI:

27   10.1126/science.1261549, 2015.

28   Chen, L., Wang, W., Wang, W., Liu, Y., Liu, F., Liu, N., and Wang, B.: Water-catalyzed

29   decomposition of the simplest Criegee intermediate $CH_2OO$, Theor. Chem. Acc., 135:131,

30   DOI 10.1007/s00214-016-1894-9, 2016.

1    Chhantyal-Pun, R., Davey, A., Shallcross, D. E., Percival, C. J., and Orr-Ewing, A. J.: A

2    kinetic study of the $CH_2OO$ Criegee intermediate self-reaction, reaction with $SO_2$ and

3    unimolecular reaction using cavity ring-down spectroscopy, Phys. Chem. Chem. Phys., 17,

4    3617-3626, 2015.

5    Chhantyal-Pun, R., Welz, O., Savee, J. D., Eskola, A. J., Lee, E. P. F., Blacker, L., Hill, H. R.,

6    Ashcroft, M., Khan, M. A. H. H., Lloyd-Jones, G. C., Evans, L. A., Rotavera, B., Huang, H.,

7    Osborn, D. L., Mok, D. K. W., Dyke, J. M., Shallcross, D. E., Percival, C. J., Orr-Ewing, A. J.

8    and Taatjes, C. A.: Direct Measurements of Unimolecular and Bimolecular Reaction Kinetics

9    of the Criegee Intermediate $(CH_3)_2COO$, J. Phys. Chem. A, 121, 4-15, 2017

10   Chuong, B., Zhang, J, and Donahue, N. M.: Cycloalkene Ozonolysis: Collisionally Mediated

11   Mechanistic Branching, J. Am. Chem. Soc., 126, 12363-12373, 2004.

12   Cox, R. A., and Penkett, S. A.: Oxidation of atmospheric $SO_2$ by products of the ozone-olefin

13   reaction, Nature, 230, 321-322, 1971.

14   Crounse, J. D., Paulot, F., Kjaergaard, H. G., and Wennberg, P. O.: Peroxy radical

15   isomerization in the oxidation of isoprene, Phys. Chem. Chem. Phys., 13, 13607-13613, 2011.

16   Crounse, J. D., Knap, H. C., Ørnsø, K. B., Jørgensen, S. Paulot, F., Kjaergaard, H. G., and

17   Wennberg, P. O.: Atmospheric fate of methacrolein. 1. Peroxy radical isomerization

18   following addition of OH and $O_2$, J. Phys. Chem. A., 116, 5756-5762, 2012.

19   Decker, Z. C. J., Au, K., Vereecken, L., and Sheps, L.: Direct experimental probing and

20   theoretical analysis of the reaction between the simplest Criegee intermediate and $CH_2OO$ and

21   isoprene, Phys. Chem. Chem. Phys., 19, 8541-8551, 2017.

22   Donahue, N. M., Drozd, G. T., Epstein, S. A., Presto, A. A., and Kroll, J. H.: Adventures in

23   ozoneland: down the rabbit-hole, Phys. Chem. Chem. Phys., 13, 10848-10857, 2011.

24   Drozd, G. T., and Donahue, N. M.: Pressure Dependence of Stabilized Criegee Intermediate

25   Formation from a Sequence of Alkenes, J. Phys. Chem. A, 115, 4381-4387, 2011.

26   Eckart, C.: The penetration of a potential barrier by electrons, Phys. Rev., 35, 1303-1309,

27   1930.

28   Ehn, M., Thornton, J. A., Kleist, E., Sipilä, M., Junninen, H., Pulli- nen, I., Springer, M.,

29   Rubach, F., Tillmann, R., Lee, B., Lopez- Hilfiker, F., Andres, S., Acir, I.-H., Rissanen, M.,

30   Jokinen, T., Schobesberger, S., Kangasluoma, J., Kontkanen, J., Nieminen, T., Kurtén, T.,

1   Nielsen, L. B., Jørgensen, S., Kjaergaard, H. G., Canagaratna, M., Maso, M. D., Berndt,

2   T., Petäjä, T., Wahner, A., Kerminen, V.-M., Kulmala, M., Worsnop, D. R., Wildt, J., and

3   Mentel, T. F.: A large source of low-volatility secondary or- ganic aerosol., Nature, 506, 476–

4   479, doi:10.1038/nature13032, 2014.

5   Fang, Y., Liu, F., Barber, V. P., Klippenstein, S. J., McCoy, A. B. and Lester, M. I.:

6   Communication: Real time observation of unimolecular decay of Criegee intermediates to OH

7   radical products, J. Chem. Phys., 144, 2016a.

8   Fang, Y., Liu, F., Klippenstein, S. J. and Lester, M. I.: Direct observation of unimolecular

9   decay of CH3CH2CHOO Criegee intermediates to OH radical products, J. Chem. Phys., 145,

10  2016b.

11  Fenske, J. D., Hasson, A. S., Ho, A. W., and Paulson, S. E.: Measurement of absolute

12  unimolecular and bimolecular rate constants for $CH_3CHOO$ generated by the trans-2-butene

13  reaction with ozone in the gas phase, J. Phys. Chem. A, 104, 9921–9932, 2000.

14  Foreman, E. S., Kapnas, K. M., and Murray, C.: Reactions between Criegee Intermediates and

15  the Inorganic Acids HCl and HNO3: Kinetics and Atmospheric Implications, Angew. Chem.

16  Int. Ed., 55, 1 – 5, 2016.

17  Frisch, M. J., Trucks, G. W., Schlegel, H. B., Scuseria, G. E., Robb, M. A., Cheeseman, J. R.,

18  Scalmani, G., Barone, V., Mennucci, B., Petersson, G. A., Nakatsuji, H., Caricato, M., Li, X.,

19  Hratchian, H. P., Izmaylov, A. F., Bloino, J., Zheng, G., Sonnenberg, J. L., Hada, M., Ehara,

20  M., Toyota, K., Fukuda, R., Hasegawa, J., Ishida, M., Nakajima, T., Honda, Y., Kitao, O.,

21  Nakai, H., Vreven, T., Montgomery Jr., J. A., Peralta, J. E., Ogliaro, F., Bearpark, M., Heyd,

22  J. J., Brothers, E., Kudin, K. N., Staroverov, V. N., Keith, T., Kobayashi, R., Normand, J.,

23  Normand, J., Raghavachari, K., Rendell, A., Burant, J. C., Iyengar, S. S., Tomasi, J., Cossi,

24  M., Rega, N., Millam, J. M., Klene, M., Knox, J. E., Cross, J. B., Bakken, V., Adamo, C.,

25  Jaramillo, J., Gomperts, R., Stratmann, R. E., Yazyev, O., Austin, A. J., Cammi, R., Pomelli,

26  C., Ochterski, J. W., Martin, R. L., Morokuma, K., Zakrzewski, V. G., Voth, G. A., Salvador,

27  P., Dannenberg, J. J., Dapprich, S., Daniels, A. D., Farkas, O., Foresman, J. B., Ortiz, J. V.,

28  Cioslowski, J., Fox, D. J. and Pople, J. A.: Gaussian 09, Revision B.01, Gaussian Inc.,

29  Wallington CT., 2010.

Atmospheric
Chemistry
and Physics
Discussions

1    Gravestock, T. J., Blitz, M. A., Bloss, W. J., and Heard, D. E.: A multidimensional study of

2    the reaction $CH_2I+O_2$: Products and atmospheric implications, ChemPhysChem, 11, 3928 –

3    3941, 2010.

4    Guenther, A., Karl, T., Harley, P., Wiedinmyer, C., Palmer, P. I., and Geron, C.: Estimates of

5    global terrestrial isoprene emissions using MEGAN (Model of Emissions of Gases and

6    Aerosols from Nature), Atmos. Chem. Phys., 6, 3181-3210, 2006.

7    Guenther, A. B., Jiang, X., Heald, C. L., Sakulyanontvittaya, T., Duhl, T., Emmons, L. K.,

8    and Wang, X.: The Model of Emissions of Gases and Aerosols from Nature version 2.1

9    (MEGAN2.1): an extended and updated framework for modeling biogenic emissions, Geosci.

10   Model Dev., 5, 1471-1492, 2012.

11   Gutbrod, R., Schindler, R. N., Kraka, E, and Cremer, D.: Formation of OH radicals in the gas

12   phase ozonolysis of alkenes: the unexpected role of carbonyl oxides, Chem. Phys. Lett., 252,

13   221–229, 1996.

14   Hackenberg S. C., Andrews, S. J., Airs, R. L., Arnold, S. R., Bouman, H. A., Cummings, D.,

15   Lewis, A. C., Minaeian, J. K., Reifel, K. M., Small, A., Tarran, G. A., Tilstone, G. H., and

16   Carpenter, L. J.: Basin-Scale Observations of Monoterpenes in the Arctic and Atlantic

17   Oceans, Environ. Sci. Technol., 51, 10449−10458, 2017.

18   Hasson, A. S., Ho, A. W., Kuwata, K. T., and Paulson, S. E.: Production of stabilized Criegee

19   intermediates and peroxides in the gas phase ozonolysis of alkenes 2. Asymmetric and

20   biogenic alkenes, J. Geophys. Res., 106, 34143–34153, 2001.

21   Hatakeyama, S., Kobayashi, H., and Akimoto, H.: Gas-Phase Oxidation of $SO_2$ in the Ozone-

22   Olefin Reactions, J. Phys. Chem., 88, 4736-4739, 1984.

23   Huang, H. -L., Chao, W., and Lin, J. J. -M.: Kinetics of a Criegee intermediate that would

24   survive at high humidity and may oxidize atmospheric $SO_2$, Proc. Natl. Acad. Sci., 112,

25   10857–10862, 2015.

26   IUPAC Task Group on Atmospheric Chemical Kinetic Data Evaluation – Data Sheet

27   Ox_VOC20, (http://iupac.pole-ether.fr), 2013.

28   Jalan, A., Allen, J. W., and Green, W. H.: Chemically activated formation of organic acids in

29   reactions of the Criegee intermediate with aldehydes and ketones, Phys. Chem. Chem. Phys.,

30   15, 16841-16852, 2013.

1  Jenkin, M. E., Saunders, S. M., and Pilling, M. J.: The tropospheric degradation of volatile

2  organic compounds: a protocol for mechanism development, Atmos. Environ., 31, 81–104,

3  1997.

4  Jenkin, M. E., Young, J. C., and Rickard, A. R.: The MCM v3.3.1 degradation scheme for

5  isoprene, Atmos. Chem. Phys., 15, 11433-11459, 2015.

6  Jiang, L., Lan, R., Xu, Y. -S., Zhang, W. -J., Yang, W.: Reaction of stabilized criegee

7  intermediates from ozonolysis of limonene with water: Ab initio and DFT study, Int. J. Mol.

8  Sci., 14, 5784-5805, 2013.

9  Johnson, D. and Marston, G.: The gas-phase ozonolysis of unsaturated volatile organic

10  compounds in the troposphere, Chem. Soc. Rev., 37, 699–716, 2008.

11  Johnston, H. S. and Heicklen, J.: Tunneling corrections for unsymmetrical Eckart potential

12  energy barriers, J. Phys. Chem., 66, 532–533, 1962.

13  Kidwell, N. M., Li, H., Wang, X., Bowman, J. M., and Lester, M. I.: Unimolecular

14  dissociation dynamics of vibrationally activated $CH_3CHOO$ Criegee intermediates to OH

15  radical products, Nature Chemistry, 8, 509-514, 2016.

16  Kirkby, J., et al.: Ion-induced nucleation of pure biogenic particles, Nature, 533, 521-526,

17  2016.

18  Kjaergaard, H. G., Kurtén, T., Nielsen, L. B., Jørgensen, S., and Wennberg, P. O.: Criegee

19  Intermediates React with Ozone, J. Phys. Chem. Lett., 4, 2525-2529, 2013.

20  Kotzias, D., Fytianos, K., and Geiss, F.: Reactions of monoterpenes with ozone, sulphur

21  dioxide and nitrogen dioxide – Gas phase oxidation of $SO_2$ and formation of sulphuric acid,

22  Atmos. Environ., 24, 2127-2132, 1990.

23  Kroll, J., Donahue, N. M., Cee, V. J., Demerjian, K. L., and Anderson, J. G.: Gas-phase

24  ozonolysis of alkenes: formation of OH from anti carbonyl oxides, J. Am. Chem. Soc., 124,

25  8518–8519, 2002.

26  Kuwata, K. T., Guinn, E., Hermes, M. R., Fernandez, J., Mathison, J. and Huang, K.: A

27  Computational Re-Examination of the Criegee Intermediate-Sulfur Dioxide Reaction, J. Phys.

28  Chem. A, 119, 10316-10335, 2015.

1  Kuwata, K. T., Hermes, M. R., Carlson, M. J., and Zogg, C. K.: Computational Studies of

2  the Isomerization and Hydration Reactions of Acetaldehyde Oxide and Methyl Vinyl

3  Carbonyl Oxide, J. Phys Chem. A, 114, 9192-9204, 2010.

4  Lelieveld, J., Butler, T. M., Crowley, J. N., Dillon, T. J., Fischer, H., Ganzeveld, L., Harder,

5  H., Lawrence, M. G., Martinez, M., Taraborrelli, D., and Williams, J.: Atmospheric oxidation

6  capacity sustained by a tropical forest, Nature, 452, 737-740, 2008.

7  Leungsakul, S., Jaoui, M., and Kamens, R. M.: Kinetic Mechanism for Predicting Secondary

8  Organic Aerosol Formation from the Reaction of *d*-limonene with Ozone, Environ. Sci.

9  Technol., 39, 9583-9594, 2005.

10  Lewis, T. R., Blitz, M. A., Heard, D. E., and Seakins, P. W.: Direct evidence for a substantive

11  reaction between the Criegee intermediate, $CH_2OO$, and the water vapour dimer, Phys. Chem.

12  Chem. Phys., 17, 4859-4863, 2015.

13  Lin, L., Chang, H., Chang, C., Chao, W., Smith, M. C., Chang, C., Lin, J. J., and Takahashi,

14  K.: Competition between $H_2O$ and $(H_2O)_2$ reactions with $CH_2OO/CH_3CHOO$, Phys. Chem.

15  Chem. Phys., 18, 4557-4568, 2016.

16  Long, B., Bao, J. L. and Truhlar, D. G.: Atmospheric Chemistry of Criegee Intermediates.

17  Unimolecular Reactions and Reactions with Water, J. Am. Chem. Soc., 138, 14409-14422,

18  2016.

19  Luo, G., and Yu, F.: A numerical evaluation of global oceanic emissions of α-pinene and

20  isoprene, Atmos. Chem. Phys., 10, 2007–2015, 2010.

21  Ma, Y., Russell, A. T., and Marston, G.: Mechanisms for the formation of secondary organic

22  aerosol components from the gas-phase ozonolysis of α-pinene, Phys. Chem. Chem. Phys.,

23  10, 4294-4312, 2008.

24  Ma, Y., and Marston, G.: Multi-functional acid formation from the gas-phase ozonolysis of β-

25  pinene, Phys. Chem. Chem. Phys., 10, 6115-6126, 2008.

26  Mao, J., Jacob, D. J., Evans, M. J., Olson, J. R., Ren, X., Brune, W. H., St. Clair, J. M.,

27  Crounse, J. D., Spencer, Beaver, M. R., Wennberg, P. O., Cubison, M. J., Jimenez, J. L.,

28  Fried, A., Weibring, P., Walega, J. G., Hall, S. R., Weinheimer, A. J., Cohen, R. C., Chen, G.,

29  Crawford, J. H., Jaeglé, L., Fisher, J. A., Yantosca, R. M., Le Sager, P., and Carouge,

Atmospheric
Chemistry
and Physics
Discussions

C.: Chemistry of hydrogen oxide radicals (HOx) in the Arctic troposphere in spring, Atmos. Chem. Phys., 10, 5823-5838, 2010.

Mao, J., Paulot, F., Jacob, D. J., Cohen, R. C., Crounse, J. D., Wennberg, P. O., Keller, C. A., Hudman, R. C., Barkley, M. P., and Horowitz, L. W.: Ozone and organic nitrates over the eastern United States: Sensitivity to isoprene chemistry, J. Geophys. Res., 118, 11256–11268, 2013.

Martinez, R. I., and Herron, J. T.: Stopped-flow studies of the mechanisms of alkene-ozone reactions in the gas-phase: tetramethylethylene, J. Phys. Chem., 91, 946-953, 1987.

Mauldin III, R. L., Berndt, T., Sipilä, M., Paasonen, P., Petäjä, T., Kim, S., Kurtén, T., Stratmann, F., Kerminen, V.-M., and Kulmala, M.: A new atmospherically relevant oxidant, Nature, 488, 193–196, 2012.

Newland, M. J., Rickard, A. R., Alam, M. S., Vereecken, L., Muñoz, A., Ródenas, M., and Bloss, W. J.: Kinetics of stabilised Criegee intermediates derived from alkene ozonolysis: reactions with $SO_2$, $H_2O$ and decomposition under boundary layer conditions, Phys. Chem. Chem. Phys., 17, 4076, 2015a.

Newland, M. J., Rickard, A. R., Vereecken, L., Muñoz, A., Ródenas, M., and Bloss, W. J.: Atmospheric isoprene ozonolysis: impacts of stabilised Criegee intermediate reactions with $SO_2$, $H_2O$ and dimethyl sulfide, Atmos. Chem. Phys., 15, 9521–9536, 2015b.

Nguyen, T. L., Peeters, J., and Vereecken, L.: Theoretical study of the gas-phase ozonolysis of β-pinene ($C_{10}H_{16}$), Phys. Chem. Chem. Phys., 11, 5643–5656, 2009a.

Nguyen, T. L., Winterhalter, R., Moortgat, G., Kanawati, B., Peeters, J., and Vereecken, L.: The gas-phase ozonolysis of β-caryophyllene ($C_{15}H_{24}$). Part II: A theoretical study, Phys. Chem. Chem. Phys., 11, 4173–4183, 2009b.

Nguyen, T. L., Lee, H., Matthews, D. A., McCarthy, M. C. and Stanton, J. F.: Stabilization of the Simplest Criegee Intermediate from the Reaction between Ozone and Ethylene: A High Level Quantum Chemical and Kinetic Analysis of Ozonolysis, J. Phys. Chem. A, 119, 5524-5533, 2015.

Niki, H., Maker, P. D., Savage, C. M., Breitenbach, L. P., and Hurley, M. D.: FTIR spectroscopic study of the mechanism for the gas-phase reaction between ozone and tetramethylethylene, J. Phys. Chem., 91, 941–946, 1987.

1  Novelli, A., Vereecken, L., Lelieveld, J., and Harder, H.: Direct observation of OH formation

2  from stabilised Criegee intermediates, Phys. Chem. Chem. Phys., 16, 19941–19951, 2014.

3  Parrella, J. P., Jacob, D. J., Liang, Q., Zhang, Y., Mickley, L. J., Miller, B., Evans, M. J.,

4  Yang, X., Pyle, J. A., Theys, N., and Van Roozendael, M.: Tropospheric bromine chemistry:

5  implications for present and pre-industrial ozone and mercury, Atmos. Chem. Phys., 12,

6  6723-6740, 2012.

7  Paulot, F., Crounse, J. D., Kjaergaard, H. G., Kürten, A., Clair, J. M. S., Seinfeld, J. H., and

8  Wennberg, P. O.: Unexpected epoxide formation in the gas-phase photooxidation of isoprene,

9  Science, 325, 730-733, 2009a.

10  Paulot, F., Crounse, J. D., Kjaergaard, H. G., Kroll, J. H., Seinfeld, J. H., and Wennberg, P.

11  O.: Isoprene photooxidation: New insights into the production of acids and organic nitrates,

12  Atmos. Chem. Phys., 9, 1479-1501, 2009b.

13  Paulson, S. E., Chung, M., Sen, A. D., and Orzechowska, G.: Measurement of OH radical

14  formation from the reaction of ozone with several biogenic alkenes, Geophys. Res. Lett., 24,

15  3193–3196, 1997.

16  Peeters, J., Nguyen, T. L., and Vereecken, L.: HOx radical regeneration in the oxidation of

17  isoprene, Phys. Chem. Chem. Phys., 11, 5935-5939, 2009.

18  Peeters, J., and Müller, J. F.: HOx radical regeneration in isoprene oxidation via peroxy

19  radical isomerisations. II: Experimental evidence and global impact, Phys. Chem. Chem.

20  Phys., 12, 14227-14235, 2010.

21  Peñuelas, J., and Staudt, M.: BVOCs and global change, Trends Plant Sci., 15, 133–144,

22  2010.

23  Pöschl, U., and Shiraiwa, M.: Multiphase Chemistry at the Atmosphere-Biosphere Interface

24  Influencing Climate and Public Health in the Anthropocene, Chem. Rev., 115, 4440–4475,

25  2015.

26  Rickard, A. R., Johnson, D., McGill, C. D., and Marston, G.: OH Yields in the Gas-Phase

27  reactions of Ozone with Alkenes, J. Phys. Chem. A, 103, 7656–7664, 1999.

28  Rossignol, S., Rio, C., Ustache, A., Fable, S., Nicolle, J., Même, A., D'Anna, B., Nicolas, M.,

29  Leoz, E., and Chiappini, L.: The use of a housecleaning product in an indoor environment

leading to oxygenated polar compounds and SOA formation: Gas and particulate phase chemical characterization, Atmos. Environ., 75, 196-205, 2013.

Ryzhkov, A. B., and P. A. Ariya, A theoretical study of the reactions of parent and substituted Criegee intermediates with water and the water dimer, Phys. Chem. Chem. Phys., 6, 5042-5050, 2004.

Sarwar, G., and Corsi, R.: The effects of ozone/limonene reactions on indoor secondary organic aerosols, Atmos. Environ., 41, 959–973, 2007.

Saunders, S. M., Jenkin, M. E., Derwent, R. G., and Pilling, M. J.: Protocol for the development of the Master Chemical Mechanism, MCM v3 (Part A): Tropospheric degradation of non-aromatic volatile organic compounds, Atmos. Chem. Phys., 3, 161-180, 2003.

Shallcross, D. E., Taatjes, C. A., and Percival, C. J.: Criegee intermediates in the indoor environment: new insights, Indoor Air, 24, 495–502, 2014.

Sheps, L., Scully, A. M., and Au, K.: UV absorption probing of the conformer-dependent reactivity of a Criegee intermediate $CH_3CHOO$ Phys. Chem. Chem. Phys., 16, 26701-26706, 2014.

Sindelarova, K., Granier, C., Bouarar, I., Guenther, A., Tilmes, S., Stavrakou, T., Müller, J.-F., Kuhn, U., Stefani, P., and Knorr, W.: Global data set of biogenic VOC emissions calculated by the MEGAN model over the last 30 years, Atmos. Chem. Phys., 14, 9317-9341, 2014.

Singer, B. C., Coleman, B. K., Destaillats, H., Hodgson, A. T., Lunden, M. M., Weschler, C. J., and Nazaroff, W. W.: Indoor secondary pollutants from cleaning product and air freshener use in the presence of ozone, Atmos. Environ., 40, 6696-6710, 2006a.

Singer, B. C., Destaillats, H., Hodgson, A. T., and Nazaroff, W. M.: Cleaning products and air fresheners: emissions and resulting concentrations of glycol ethers and terpenoids, Indoor Air, 16, 179-191, 2006b.

Sipilä, M., Jokinen, T., Berndt, T., Richters, S., Makkonen, R., Donahue, N. M., Mauldin III, R. L., Kurtén, T., Paasonen, P., Sarnela, N., Ehn, M., Junninen, H., Rissanen, M. P., Thornton, J., Stratmann, F., Herrmann, H., Worsnop, D. R., Kulmala, M., Kerminen, V.-M., and Petäjä, T.: Reactivity of stabilized Criegee intermediates (sCIs) from

1   isoprene and monoterpene ozonolysis toward $SO_2$ and organic acids, Atmos. Chem. Phys., 14,

2   12143-12153, 2014.

3   Smith, M. C., Chao, W., Takahashi, K., Boering, K. A., and Lin, J. J. -M.: Unimolecular

4   Decomposition Rate of the Criegee Intermediate $(CH_3)_2COO$ Measured Directly with UV

5   Absorption Spectroscopy, J. Phys. Chem. A, doi: 10.1021/acs.jpca.5b12124, 2016.

6   Stone, D., Blitz, M., Daubney, L., Howes, N. U. M., and Seakins, P.: Kinetics of $CH_2OO$

7   reactions with $SO_2$, $NO_2$, NO, $H_2O$, and $CH_3CHO$ as a function of pressure, Phys. Chem.

8   Chem. Phys., 16, 1139-1149, 2014.

9   Su, Y. -T., Lin, H. -Y., Putikam, R., Matsui, H., Lin, M. C., and Lee, Y. -P.: Extremely rapid

10   self-reaction of the simplest Criegee intermediate $CH_2OO$ and its implications in atmospheric

11   chemistry, Nature Chemistry, 6, 477-483, 2014.

12   Taatjes, C. A., Welz, O., Eskola, A. J., Savee, J. D., Osborn, D. L., Lee, E. P. F., Dyke, J. M.,

13   Mok, D. W. K., Shallcross, D. E., and Percival, C. J.: Direct measurements of Criegee

14   intermediate $(CH_2OO)$ formed by reaction of $CH_2I$ with $O_2$, Phys. Chem. Chem. Phys., 14,

15   10391-10400, 2012.

16   Taatjes, C. A., Welz, O., Eskola, A. J., Savee, J. D., Scheer, A. M., Shallcross, D. E.,

17   Rotavera, B., Lee, E. P. F., Dyke, J. M., Mok, D. K. W., Osborn, D. L., and Percival, C. J.:

18   Direct Measurements of Conformer-Dependent Reactivity of the Criegee Intermediate

19   $CH_3CHOO$, Science, 340, 177–180, 2013.

20   Taatjes, C. A., Shallcross, D. E., and Percival, C. J.: Research frontiers in the chemistry of

21   Criegee intermediates and tropospheric ozonolysis, Phys. Chem. Chem. Phys., 16, 1704-1718,

22   2014.

23   Taipale, R., Sarnela, N., Rissanen, M., Junninen, H., Rantala, P., Korhonen, F., Siivola, E.,

24   Berndt, T., Kulmala, M., Mauldin, R.L. III, Petäjä, T., Sipilä, M.: New instrument for

25   measuring atmospheric concentrations of non-OH oxidants of $SO_2$, Bor. Env. Res., 19 (suppl.

26   B), 55-70, 2014.

27   Truhlar, D. G., Garrett, B. C. and Klippenstein, S. J.: Current Status of Transition-State

28   Theory, J. Phys. Chem., 100, 12771-12800, 1996.

Atmospheric
Chemistry
and Physics
Discussions

1   Vereecken, L. and Peeters, J.: The 1,5-H-shift in 1-butoxy: A case study in the rigorous

2   implementation of transition state theory for a multirotamer system, J. Chem. Phys., 119,

3   5159-5170, 2003.

4   Vereecken, L., and Francisco, J. S.: Theoretical studies of atmospheric reaction mechanisms

5   in the troposphere, Chem. Soc. Rev., 41, 6259-6293, 2012.

6   Vereecken, L., Harder, H., and Novelli, A.: The reaction of Criegee intermediates with NO,

7   $RO_2$, and $SO_2$, and their fate in the atmosphere, Phys. Chem. Chem. Phys., 14, 14682–14695,

8   2012.

9   Vereecken, L., Harder, H., and Novelli, A.: The reactions of Criegee intermediates with

10  alkenes, ozone and carbonyl oxides, Phys. Chem. Chem. Phys., 16, 4039–4049, 2014.

11  Vereecken, L., Rickard, A. R., Newland, M. J., and Bloss, W. J.: Theoretical study of the

12  reactions of Criegee intermediates with ozone, alkylhydroperoxides, and carbon monoxide,

13  Phys. Chem. Chem. Phys., 17, 23847–23858, 2015.

14  Vereecken, L., and Nguyen, H. M. T.: Theoretical Study of the Reaction of Carbonyl Oxide

15  with Nitrogen Dioxide: $CH_2OO$ + $NO_2$, Int. J. Chem. Kinet., 49, 752-760, 2017.

16  Vereecken, L.: The Reaction of Criegee Intermediates with Acids and Enols, Phys. Chem.

17  Chem. Phys., DOI: 10.1039/C7CP05132H, 2017.

18  Vereecken, L., Novelli, A., and Taraborrelli, D.: Unimolecular decay strongly limits

19  concentration of Criegee intermediates in the atmosphere, Manuscript in preparation, 2017.

20  Wang, L., and Wang, L.: Mechanism of gas-phase ozonolysis of sabinene in the atmosphere,

21  Phys. Chem. Chem. Phys., doi: 10.1039/c7cp03216a, 2017.

22  Wei, W., Zheng, R., Pan, Y., Wu, Y., Yang, F., and Hong, S.: Ozone Dissociation to

23  Oxygen Affected by Criegee Intermediate, J. Phys. Chem. A, 118, 1644–1650, 2014.

24  Wei, W. -M., Yang, X., Zheng, R. -H., Qin, Y. -D., Wu, Y. -K., Yang, F.: Theoretical studies

25  on the reactions of the simplest Criegee intermediate $CH_2OO$ with $CH_3CHO$, Comp. Theor.

26  Chem., 1074, 142-149, 2015.

27  Welz, O., Eskola, A. J., Sheps, L., Rotavera, B., Savee, J. D., Scheer, A. M., Osborn, D. L.,

28  Lowe, D., Murray Booth, A., Xiao, P., Anwar H., Khan, M., Percival, C. J., Shallcross, D. E.,

29  and Taatjes, C. A.: Rate coefficients of C1 and C2 Criegee intermediate reactions with formic

Atmospheric
Chemistry
and Physics
Discussions

1  and acetic acid near the collision limit: direct kinetics measurements and atmospheric

2  implications, Angew. Chem. Int. Ed. Engl., 53, 4547–4750, 2014.

3  Welz, O., Savee, J. D., Osborn, D. L., Vasu, S. S., Percival, C. J., Shallcross, D. E., and

4  Taatjes, C. A.: Direct Kinetic Measurements of Criegee Intermediate ($CH_2OO$) Formed by

5  Reaction of $CH_2I$ with $O_2$, Science, 335, 204–207, 2012.

6  Winterhalter, R., Neeb, P., Grossmann, D., Kolloff, A., Horie, O., and Moortgat, G.: Products

7  and Mechanism of the Gas Phase Reaction of Ozone with β-pinene, J. Atmos. Chem., 35,

8  165-197, 2000.

9  Yao, L., Ma, Y., Wang, L., Zheng, J., Khalizov, A., Chen, M., Zhou, Y., Qi, L., and Cui, F.:

10  Role of stabilized Criegee Intermediate in secondary organic aerosol formation from the

11  ozonolysis of α-cedrene, Atmos. Environ., 94, 448-457, 2014.

12  Zhang, D., and Zhang, R.: Ozonolysis of α-pinene and β-pinene: Kinetics and mechanism, J.

13  Chem. Phys., 122, 114308, 2005.

14  Zhang, J., Huff Hartz, K. E., Pandis, S. N., and Donahue, N. M.: Secondary Organic Aerosol

15  Formation from Limonene Ozonolysis: Homogeneous and Heterogeneous Influences as a

16  Function of $NO_x$, J. Phys. Chem. A, 110, 11053-11063, 2006.

17  Zhou, L., Gierens, R., Sogachev, A., Mogensen, D., Ortega, J., Smith, J. N., Harley, P. C.,

18  Prenni, A. J., Levin, E. J. T., Turnipseed, A., Rusanen, A., Smolander, S., Guenther, A. B.,

19  Kulmala, M., Karl, T., and Boy, M.: Contribution from biogenic organic compounds to

20  particle growth during the 2010 BEACHON-ROCS campaign in a Colorado temperate needle

21  leaf forest, Atmos. Chem. Phys. Discuss., 15, 9033-9075, doi:10.5194/acpd-15-9033-2015,

22  2015.

23

24

25

Atmospheric
Chemistry
and Physics
Discussions

Open Access

EGU

1    Table 1. Monoterpene SCI yields derived in this work and reported in the literature.

| $\phi_{SCI}$ | Reference | Notes | Methodology |
|---|---|---|---|
| **α-pinene** | | | |
| 0.19 (± 0.01) | This work | | $SO_2$ loss |
| 0.15 (± 0.07) | Sipilä et al. (2014) | | Formation of $H_2SO_4$ |
| 0.22 | Taipale et al. (2014) (personal comm. Berndt) | | |
| 0.125 (± 0.04) | Hatakeyama et al. (1984) | | Formation of $H_2SO_4$ |
| 0.20 | MCMv3.3.1 [a] | | |
| **β-pinene** | | | |
| 0.60 (± 0.03) | This work | | $SO_2$ loss |
| 0.46 | Ahrens et al. (2014) | $\phi_{C9-SCI}$: 0.36  $\phi_{CH2OO}$: 0.10 | FTIR detection |
| 0.25 | MCMv3.3.1 [a] | $\phi_{C9-SCI}$: 0.102  $\phi_{CH2OO}$: 0.148 | |
| 0.42 | Nguyen et al. (2009) | $\phi_{C9-SCI}$: 0.37  $\phi_{CH2OO}$: 0.05 | Theoretical |
| 0.51 | Winterhalter et al. (2000) | $\phi_{C9-SCI}$: 0.35  $\phi_{CH2OO}$: 0.16 | Change in nopinone yields $f([H_2O])$ |
| 0.44 | Kotzias et al. (1990) | | Formation of $H_2SO_4$ |
| 0.25 | Hatakeyama et al. (1984) | | Formation of $H_2SO_4$ |
| 0.30 | Zhang and Zhang (2005) | $\phi_{C9-SCI}$: 0.22  $\phi_{CH2OO}$: 0.08 | |
| > 0.27 | Ma and Marston (2008) | $\phi_{C9-SCI}$: 0.27  $\phi_{CH2OO}$: 0.16[a]  $\phi_{CH2OO}$: 0.06[b] | Change in nopinone yields $f([H_2O])$ |
| 0.27 | Hasson et al. (2001) | | Change in nopinone yields $f([H_2O])$ |
| **Limonene** | | | |
| 0.23 (± 0.01) | This work | | $SO_2$ loss |
| 0.27 (± 0.12) | Sipilä et al. (2014) | | Formation of $H_2SO_4$ |
| 0.34 | Leungsakul et al. (2005) | $\phi_{C10-SCI}$: 0.26  $\phi_{CI-x}$: 0.04  $\phi_{CH2OO}$: 0.05 | Measurement of stable particle and gas-phase products |
| 0.135 | MCMv3.3.1 [a] | | |

Atmospheric
Chemistry
and Physics

Open Access

EGU

Discussions

1    Uncertainty ranges (± 2σ, parentheses) indicate combined precision and systematic measurement error

2    components for this work, and are given as stated for literature studies. All referenced experimental studies

3    produced SCI from MT + $O_3$ and were conducted between 700 and 760 Torr. [a] http://mcm.leeds.ac.uk/MCM/

4    (Jenkin et al., 2015).

5    [a] assuming 100 % stabilisation

6    [b] assuming 40 % stabilisation

1    Table 2. Monoterpene derived SCI relative and absolute[a] rate constants derived in this work.

| SCI | $10^5\,k_3/k_2$ | $10^{15}\,k_3$ (cm$^3$ s$^{-1}$) | $10^{-12}\,k_d/k_2$ (cm$^{-3}$) | $k_d$ (s$^{-1}$) |
|---|---|---|---|---|
| *α-pinene* | | | | |
| SCI-A | > 140 (± 34) | > 310 (± 75)[a] | | |
| SCI-B | | | < 8.2 (± 1.5) | < 240 (± 44)[c] |
| *β-pinene* | | | | |
| SCI-A | > 10 (± 2.7) | > 4 (± 1)[b] | | |
| SCI-B | | | < 6.0 (± 1.3) | < 170 (± 38)[c] |
| *Limonene* | | | | |
| SCI-A | < 3.5 (± 0.2) | < 7.7 (± 0.6)[a] | | |
| SCI-B | | | > 4.5 (± 0.1) | > 130 (± 3)[c] |

2    Uncertainty ranges (± 2σ, parentheses) indicate combined precision and systematic measurement error

3    components. [a] Scaled to an absolute value using $k_2$(anti-CH$_3$CHOO) = 2.2 × 10$^{-10}$ cm$^3$ s$^{-1}$ (Sheps et al., 2014); [b]

4    Scaled to an absolute value using $k_2$(anti-CH$_3$CHOO) = 4 × 10$^{-11}$ cm$^3$ s$^{-1}$ (Ahrens et al., 2014); [c] Scaled using

5    $k_2$(syn-CH$_3$CHOO) = 2.9 × 10$^{-11}$ cm$^3$ s$^{-1}$ (Sheps et al., 2014).

6

7

8

9

10

11

12

13

1    Table 3. Unimolecular reactions for the CI derived from α-pinene, β-pinene, and *d*-limonene,

2    as derived by Vereecken et al. (2017). Barrier heights (kcal mol$^{-1}$) listed estimate post-

3    CCSD(T) energies.

| Carbonyl oxide | Reaction | $E_b$ | $k(298K) / s^{-1}$ |
|---|---|---|---|
| *α-pinene* | | | |
| CI-1a | 1,4-H-migration | 15.8 | 600 |
|  | SOZ-formation | 15.6 | $5\times10^{-2}$ |
|  | 1,3-ring closure | 21.6 | $1\times10^{-3}$ |
| CI-1b | 1,3-ring closure | 14.8 | 60 |
|  | 1,3-H-migration | 29.0 | $1\times10^{-6}$ |
| CI-2a | 1,4-H-migration | 16.3 | 250 |
|  | 1,3-ring closure | 20.8 | $6\times10^{-3}$ |
| CI-2b | 1,4-H-migration | 17.0 | 60 |
|  | SOZ-formation | 13.5 | 8 |
|  | Ring closure | 19.9 | $3\times10^{-2}$ |
| *β-pinene* | | | |
| CI-3 | 1,4-H-migration | 15.7 | 375 |
|  | 1,3-ring closure | 21.1 | $2\times10^{-3}$ |
| CI-4 | 1,3-ring closure | 17.2 | 2.0 |
|  | Ring opening | 23.6 | (Slow, Nguyen et al. 2009a) |
|  | 1,4-H-migration | 24.9 | (Slow, Nguyen et al. 2009a) |
| $CH_2OO$ | 1,3-ring closure | 19.0 | 0.3 |
|  | 1,3-H-migration | 30.7 | $1\times10^{-7}$ |
| *Limonene*[a] | | | |
| CI-5a | 1,4-H-migration | SAR | 200 [a] |
| CI-5b | 1,3-ring closure | SAR | 75 [a] |
| CI-6a | 1,4-H-migration | SAR | 430 [a] |
| CI-6b | 1,4-H-migration | SAR | 700 [a] |
| CI-7a | 1,4-H-migration | SAR | 15 |
| CI-7b | 1,4-H-migration | SAR | 600 |

4    [a] Formation of secondary ozonides (SOZ) is not included, and could be the dominant unimolecular loss.

5

6

Atmospheric
Chemistry
and Physics
Discussions

1  Table 4. Rate coefficients ($cm^3$ molecule$^{-1}$ s$^{-1}$) for the reaction of CI with $H_2O$ and $(H_2O)_2$ as

2  predicted by Vereecken et al. (2017). Values are based on explicit CCSD(T)/aug-cc-

3  pVTZ//M06-2X/aug-cc-pVTZ calculations and multi-conformer TST, including empirical

4  corrections to reference experimental data, except for limonene-derived CI where the values

5  are predicted using a structure-activity relationship. The rate coefficients for $CH_2OO$,

6  $CH_3CHOO$, and $(CH_3)_2COO$ are within a factor of 4 of evaluated literature data (Vereecken et

7  al., 2017).

| Carbonyl oxide | $k$(298K) $H_2O$ | $k$(298K) $(H_2O)_2$ |
|---|---|---|
| $CH_2OO$ | $8.7 \times 10^{-16}$ | $1.4 \times 10^{-12}$ |
| syn-$CH_3CHOO$ | $6.7 \times 10^{-19}$ | $2.1 \times 10^{-15}$ |
| anti-$CH_3CHOO$ | $2.3 \times 10^{-14}$ | $2.7 \times 10^{-11}$ |
| $(CH_3)_2COO$ | $7.5 \times 10^{-18}$ | $1.8 \times 10^{-14}$ |
| **α-pinene** | | |
| CI-1a | $1.3 \times 10^{-18}$ | $2.9 \times 10^{-15}$ |
| CI-1b | $1.5 \times 10^{-14}$ | $1.7 \times 10^{-11}$ |
| CI-2a | $1.0 \times 10^{-18}$ | $2.5 \times 10^{-15}$ |
| CI-2b | $2.4 \times 10^{-19}$ | $7.0 \times 10^{-16}$ |
| **β-pinene** | | |
| CI-3 | $1.7 \times 10^{-18}$ | $4.3 \times 10^{-15}$ |
| CI-4 | $4.2 \times 10^{-16}$ | $6.4 \times 10^{-13}$ |
| **Limonene** | | |
| CI-5a | $1.5 \times 10^{-18}$ | $4.3 \times 10^{-15}$ |
| CI-5b | $1.5 \times 10^{-14}$ | $1.7 \times 10^{-11}$ |
| CI-6a | $9.1 \times 10^{-18}$ | $2.1 \times 10^{-14}$ |
| CI-6b | $1.5 \times 10^{-17}$ | $3.2 \times 10^{-14}$ |
| CI-7a | $9.7 \times 10^{-18}$ | $1.9 \times 10^{-14}$ |
| CI-7b | $4.3 \times 10^{-18}$ | $1.1 \times 10^{-14}$ |

8

9

1    Table 5.  Kinetic parameters used in the global modelling study.

| SCI | $\phi_{SCI}$ | $10^{15}\, k_3$ (cm$^3$ s$^{-1}$) | $10^{11}\, k_2$ [a] (cm$^3$ s$^{-1}$) | $k_d$ (s$^{-1}$) |
|---|---|---|---|---|
| **α-pinene** | | | | |
| SCI-A | 0.08 | 310 | 22 | - |
| SCI-B | 0.11 | - | 2.9 | 240 |
| **β-pinene** | | | | |
| SCI-A | 0.25 | 4 | 4 | - |
| SCI-B | 0.35 | - | 2.9 | 170 |
| **Limonene** | | | | |
| SCI-A | 0.05 | 7.7 | 22 | - |
| SCI-B | 0.18 | - | 2.9 | 130 |
| **Myrcene** | | | | |
| SCI-B | 0.30 | - | 13[b] | 819[c] |
| **Ocimene** | | | | |
| SCI-B | 0.30 | - | 13[b] | 819[c] |
| **Sabinene** [d] | | | | |
| SCI-A | 0.25 | 4 | 4 | - |
| SCI-B | 0.35 | - | 2.9 | 170 |
| **3-carene** [e] | | | | |
| SCI-A | 0.08 | 310 | 22 | - |
| SCI-B | 0.11 | - | 2.9 | 240 |

2    [a] $k_2$(SCI-A+SO$_2$) from (SO$_2$+*anti*-CH$_3$CHOO) - Sheps et al. (2014); $k_2$(SCI-B+SO$_2$) from (SO$_2$+*syn*-CH$_3$CHOO)
3    - Sheps et al. (2014) unless otherwise stated
4    [b] $k_2$(SCI-B+SO$_2$) from (SO$_2$+*anti*-(CH$_3$)$_2$COO) – Huang et al. (2015)
5    [c] $k_d$(SCI-B) from Newland et al. (2015) (scaled to $k_2$(SCI-B+SO$_2$) from Huang et al. (2015)
6    [d] Kinetics based on *β*-pinene
7    [e] Kinetics based on *α*-pinene
8

1    Table 6. Monoterpene contribution to [SCI] and SO$_2$ oxidation in the surface layer of the
2    model simulation.

| Monoterpene | Annual emissions[a] (Tg C) | % contribution to [SCI-A] | % contribution to [SCI-B] | % contribution to SO$_2$ oxidation |
|---|---|---|---|---|
| α-pinene | 35.4 | 0.5 | 16 | 6.9 |
| β-pinene | 16.9 | 74 | 46 | 65 |
| limonene | 9.2 | 3.5 | 14 | 7.2 |
| myrcene | 3.1 | 0.0 | 1.2 | 4.5 |
| trans-β-ocimene | 14.1 | 0.0 | 5.4 | 11 |
| sabinene | 7.9 | 22 | 14 | 4.5 |
| 3-carene | 6.4 | 0.0 | 2.7 | 1.6 |

3    [a] From MEGAN v2.1 (Guenther et al., 2012)
4

1
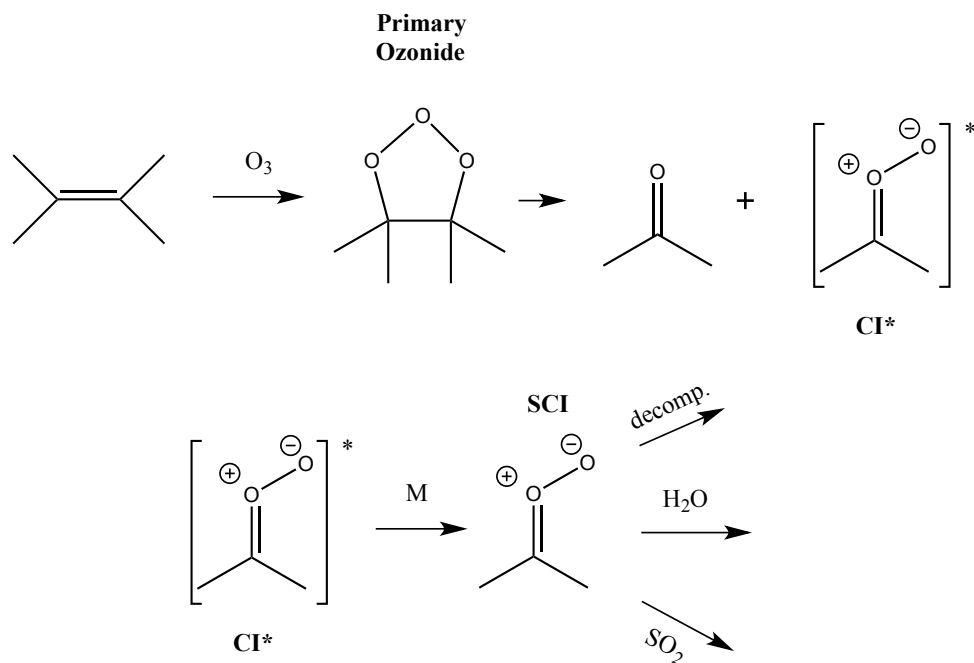


Scheme 1. Simplified generic mechanism for the reaction of Criegee Intermediates (CIs) formed from alkene ozonolysis.

2

3

4

5

6

7

8

9

10

11

12

13

14

15
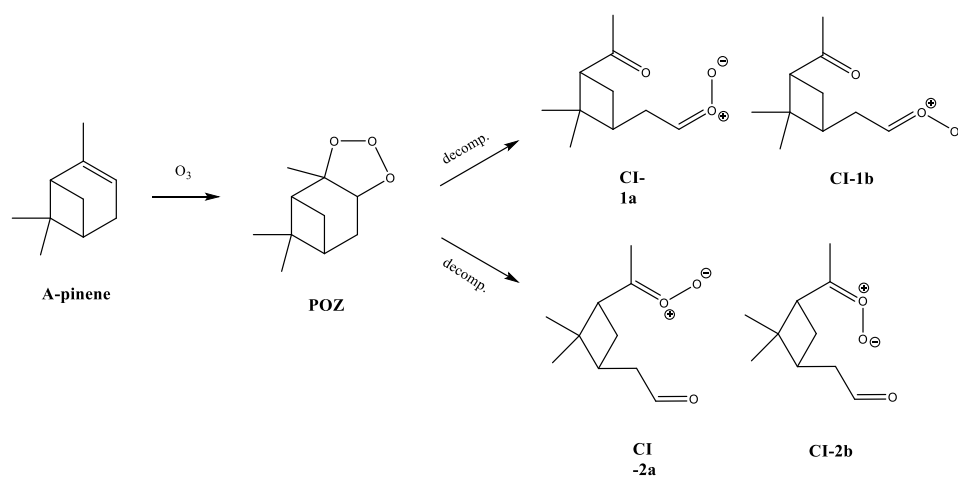
1

2

3    Scheme 2. Mechanism of formation of the two Criegee Intermediates (CIs) from α-pinene

4    ozonolysis.

5

6

7

8

9

10

Atmospheric
Chemistry
and Physics
Discussions

Open Access



1

2
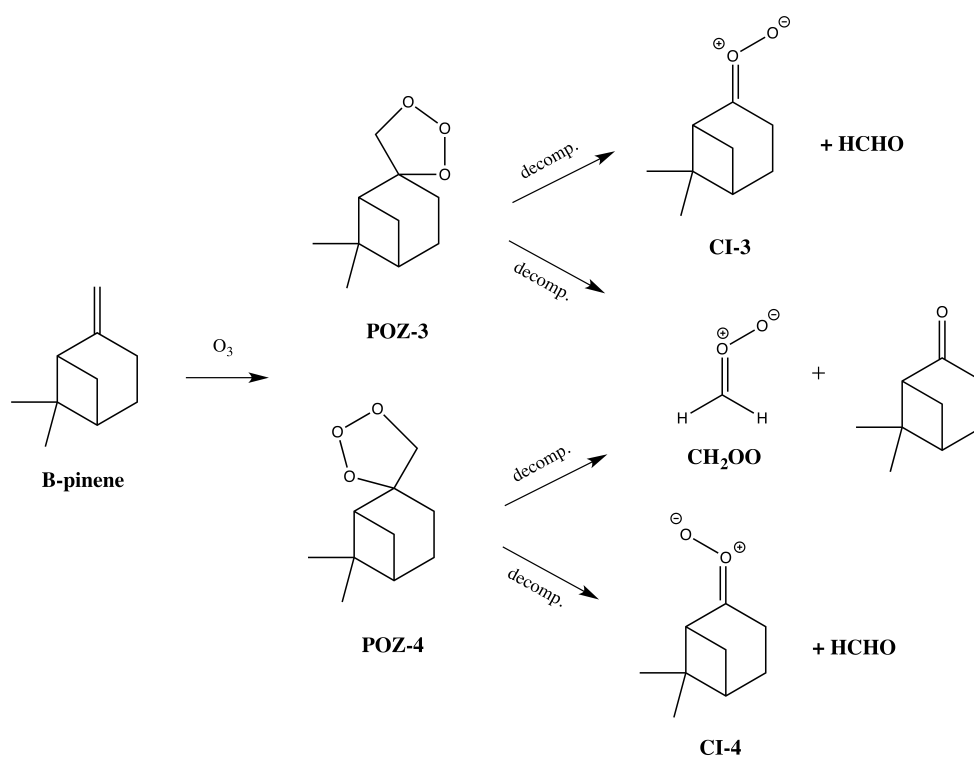
Scheme 3. Mechanism of formation of the three Criegee Intermediates (CIs) from β-pinene
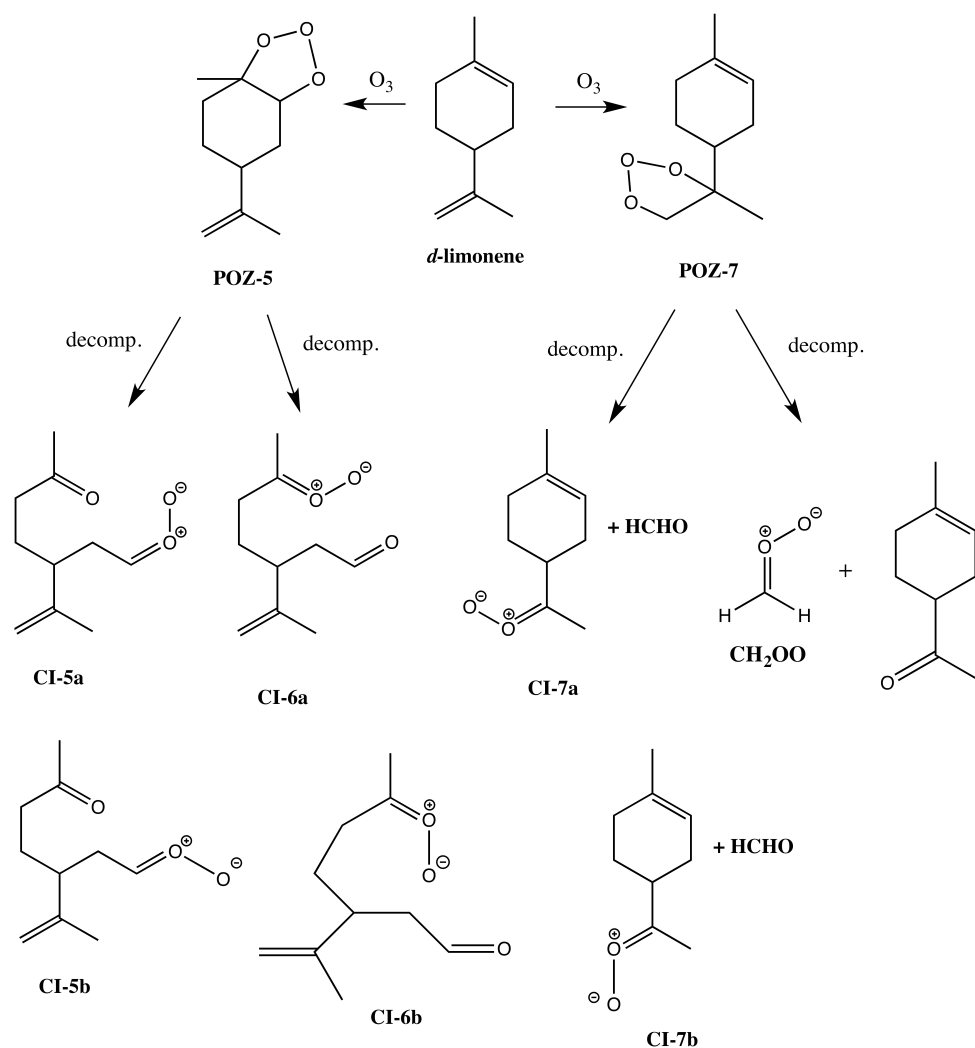
ozonolysis.

1

2

3    Scheme 4. Mechanism of formation of the four Criegee Intermediates (CIs) from limonene

4    ozonolysis.

5

Atmospheric
Chemistry
and Physics
Discussions



1
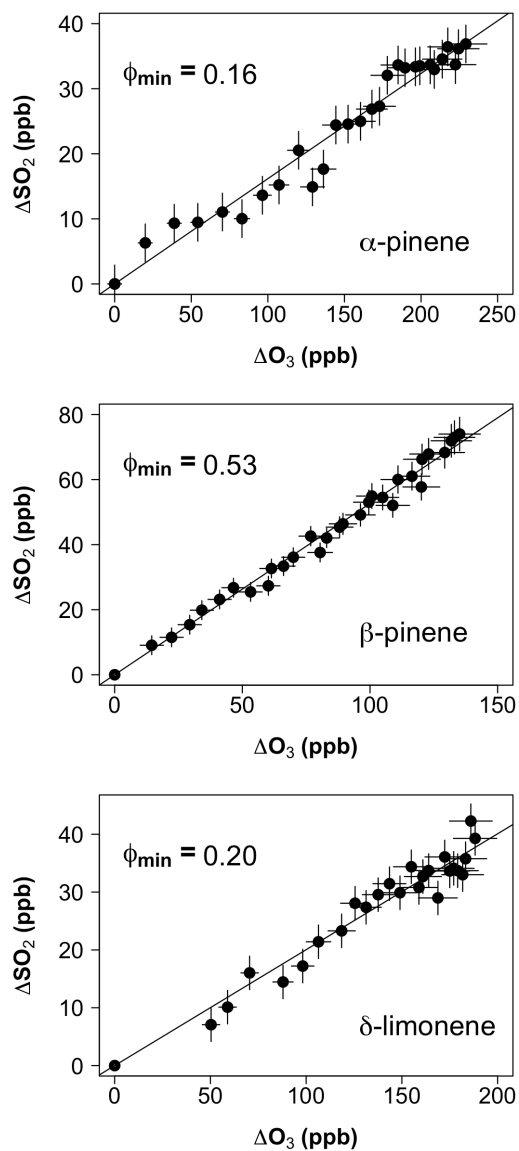
Figure 1. $\Delta SO_2$ vs. $\Delta O_3$ during excess $SO_2$ experiments ($[H_2O] < 5 \times 10^{15}$ cm$^{-3}$). The gradient

3    determines the minimum SCI yield ($\phi_{min}$).

4

1
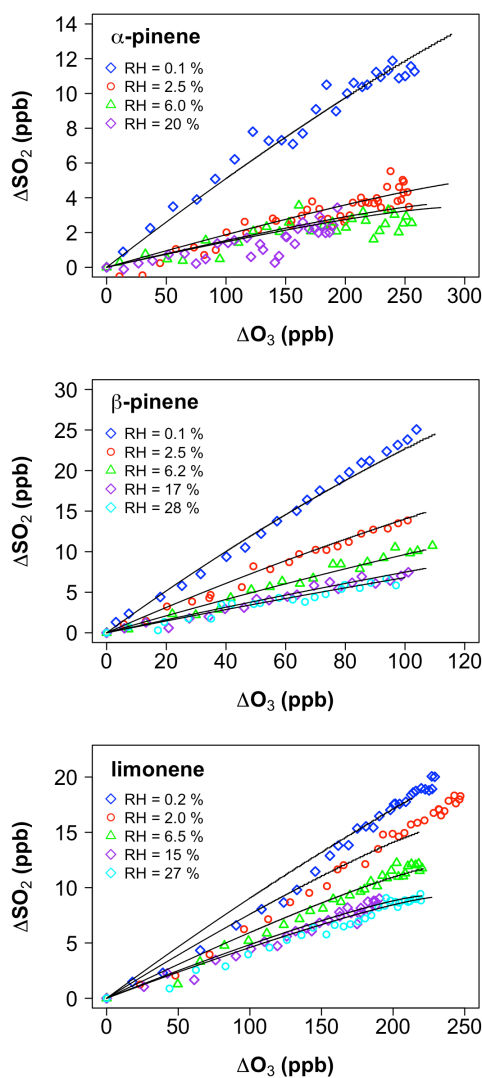
Figure 2. Cumulative consumption of $SO_2$ as a function of cumulative consumption of $O_3$,

$\Delta SO_2$ versus $\Delta O_3$, for the ozonolysis of α-pinene, β-pinene and limonene in the presence of

$SO_2$ at a range of water vapour concentrations, from $1 \times 10^{15}$ cm$^{-3}$ to $1.9 \times 10^{17}$ cm$^{-3}$. Symbols

are experimental data, corrected for chamber dilution. Lines are smoothed fits to the

experimental data.

7

Atmospheric
Chemistry
and Physics
Discussions
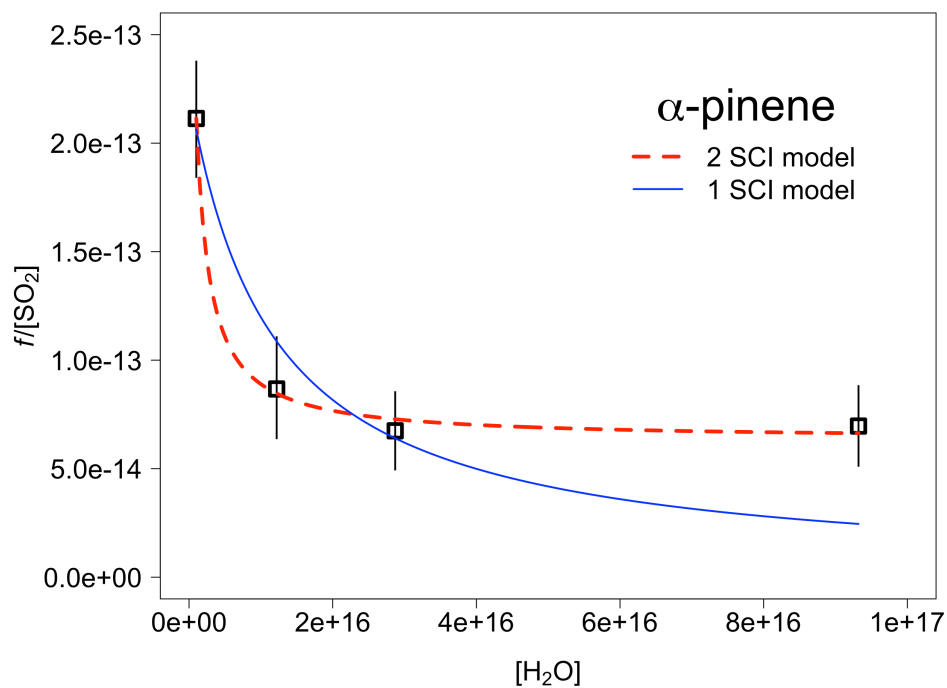


1

2   Figure 3. Application of a 2 SCI model fit (Equation E4) and a single SCI model fit (Equation

3   E1) to the measured values (open squares) of $f$/[$SO_2$] for α-pinene. From the fit we derive

4   relative rate constants for reaction of the α-pinene derived SCI, SCI-A and SCI-B with $H_2O$

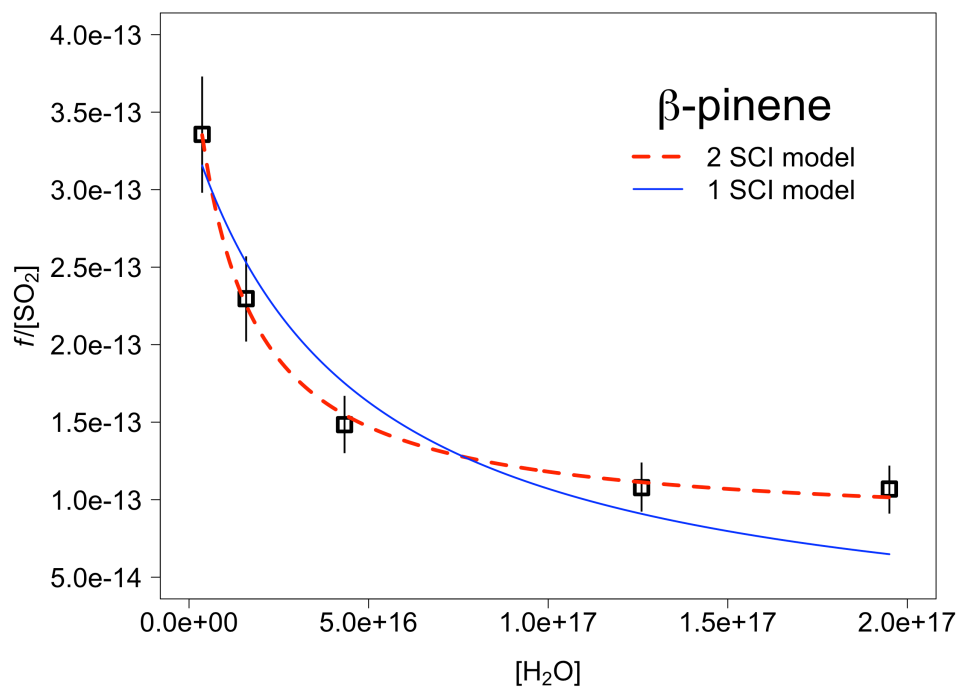5   ($k_3/k_2$) and decomposition (($k_d+L)/k_2$) assuming that $\gamma^A = 0.40$ and $\gamma^B = 0.60$.

6

7

8

9

10

Atmospheric
Chemistry
and Physics
Discussions

Open Access



1

2     Figure 4. Application of a 2 SCI model fit (Equation E4) and a single SCI model fit (Equation

3     E1) to the measured values (open squares) of $f/[SO_2]$ for β-pinene. From the fit we derive

4     relative rate constants for reaction of the β-pinene derived SCI, SCI-A and SCI-B with $H_2O$

5     $(k_3/k_2)$ and decomposition $((k_d+L)/k_2)$ assuming that $\gamma^A = 0.41$ and $\gamma^B = 0.59$.
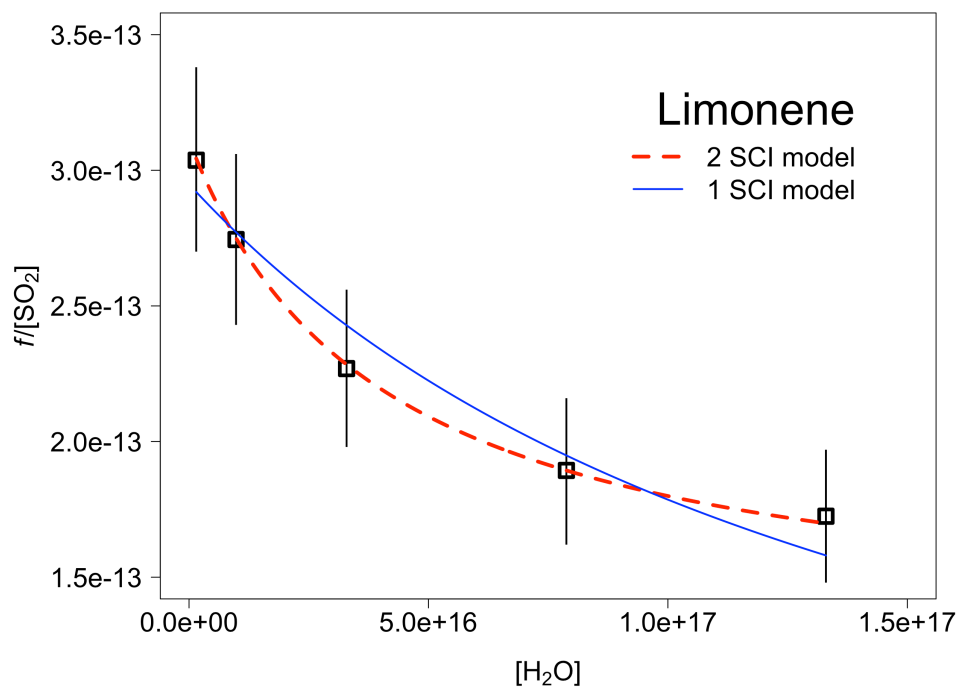
1

2

3   Figure 5. Application of a 2 SCI model fit (Equation E4) and a single SCI model fit (Equation

4   E1) to the measured values (open squares) of $f/[SO_2]$ for limonene. From the fit we derive

5   relative rate constants for reaction of the limonene derived SCI, SCI-A and SCI-B with $H_2O$

6   $(k_3/k_2)$ and decomposition $((k_d+L)/k_2)$ assuming that $\gamma^A = 0.22$ and $\gamma^B = 0.78$.
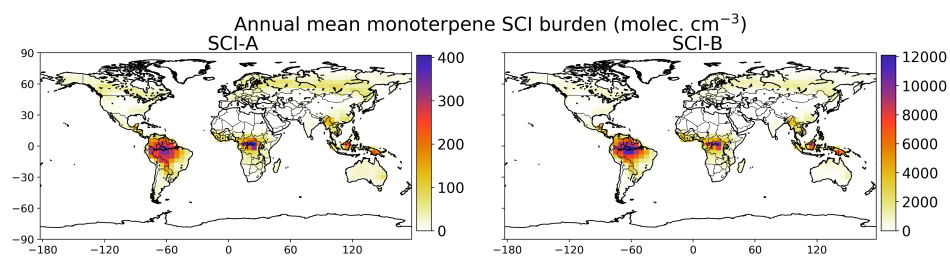
7

8

9

10

11

12

13

Atmospheric
Chemistry
and Physics
Discussions
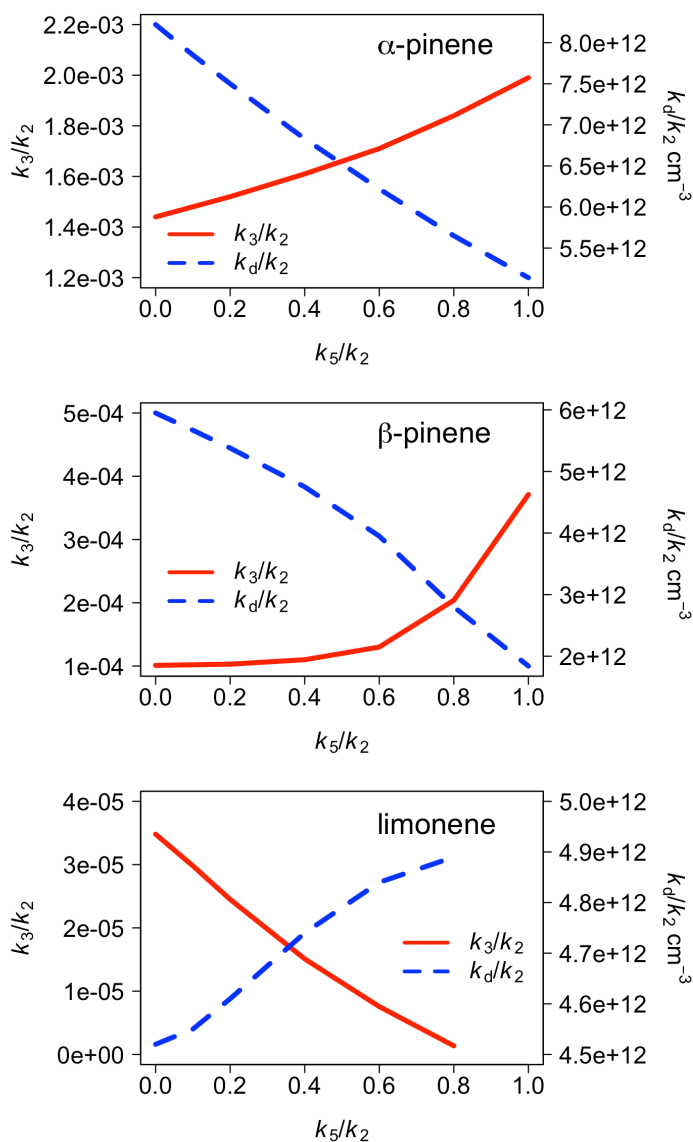


1

2  Figure 6. Variation of $k_3/k_2$ ($k$(SCI-A+H$_2$O))/($k$(SCI-A+SO$_2$)) and $k_d$ ($k$(SCI-B
3  unimol.))/($k$(SCI-B+SO$_2$)) as a function of the ratio $k_5/k_2$ ($k$(SCI+acid)/$k$(SCI+SO$_2$)), derived
4  from least squares fit of Equation E4 to measurements shown in Figures 3 -5 for α-
5  pinene, β-pinene and limonene respectively.
6
7

Figure 7. Annual mean monoterpene SCI-A and SCI-B concentrations (cm$^{-3}$) in the surface layer of the GEOS-Chem simulation.
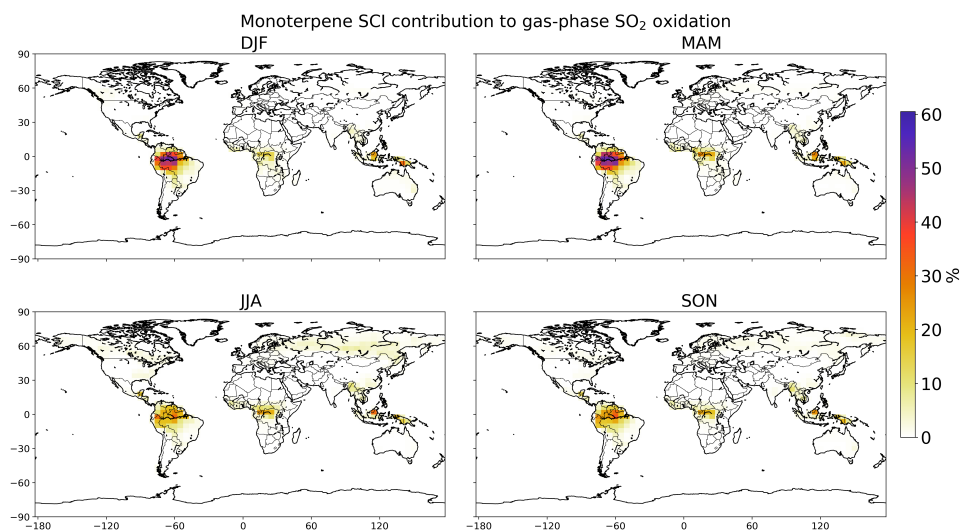
Figure 8. Seasonal SO$_2$ oxidation by monoterpene SCI as percentage of total gas-phase SO$_2$ oxidation in the surface layer.